

Accumulation and Secretion of Coumarinolignans and other Coumarins in *Arabidopsis thaliana* Roots in Response to Iron Deficiency at High pH

Patricia Sisó-Terraza¹, Adrian Luis-Villarroya¹, Pierre Fourcroy², Jean-Francois BRIAT², Anunciación Abadía¹, Frédéric Gaymard², Javier Abadía¹, Ana Álvarez-Fernández^{1*}

¹Plant Nutrition, Aula Dei Experimental Station, Consejo Superior de Investigaciones Científicas (CSIC), Spain, ²Biochimie et Physiologie Moléculaire des Plantes, Centre National de la Recherche Scientifique, Institut National de la Recherche Agronomique, Université Montpellier, France

Submitted to Journal:
Frontiers in Plant Science

Specialty Section:
Plant Physiology

Article type:
Original Research Article

Manuscript ID:
222572

Received on:
29 Jul 2016

Revised on:
26 Oct 2016

Frontiers website link:
www.frontiersin.org

Conflict of interest statement

The authors declare that the research was conducted in the absence of any commercial or financial relationships that could be construed as a potential conflict of interest

Author contribution statement

AA-F, PF and AA conceived and designed the experiments, PS-T conducted experiments, collected data, and drafted the manuscript, AL-V quantified phenolics, carried out Fe mobilization studies and made figures, AA, FG, J-FB, JA and AA-F wrote, reviewed and edited the paper. All authors read and approved the final manuscript.

Keywords

Arabidopsis, Cleomiscosin, Coumarin, Fraxetin, iron nutrition, Mass Spectrometry, Root secretion

Abstract

Word count: 333

Root secretion of coumarin-phenolic type compounds has been recently shown to be related to *Arabidopsis thaliana* tolerance to Fe deficiency at high pH. These studies revealed the identity of a few simple coumarins occurring in roots and exudates of Fe-deficient *A. thaliana* plants, and left open the possible existence of other unknown phenolics. We used HPLC-UV-VIS-ESI-MS(TOF), HPLC/ESI-MSn(ion trap) and HPLC-ESI-MS-MS(Q-TOF) to characterize (identify and quantify) phenolic-type compounds accumulated in roots or secreted into the nutrient solution of *A. thaliana* plants in response to Fe deficiency. Plants grown with or without Fe and using nutrient solutions buffered at pH 5.5 or 7.5 enabled to identify an array of phenolics. These include several coumarinolignans not previously reported in *A. thaliana* (cleomiscosins A, B, C and D and the 5'-hydroxycleomiscosins A and/or B), as well as some coumarin precursors (ferulic acid and coniferyl and sinapyl aldehydes), and previously reported catechol (fraxetin) and non-catechol coumarins (scopoletin, isofraxidin and fraxinol), some of them in hexoside forms not previously characterized. The production and secretion of phenolics were more intense when the plant accessibility to Fe was diminished and the plant Fe status deteriorated, as it occurs when plants are grown in the absence of Fe at pH 7.5. Aglycones and hexosides of the four coumarins were abundant in roots, whereas only the aglycone forms could be quantified in the nutrient solution. A comprehensive quantification of coumarins, first carried out in this study, revealed that the catechol coumarin fraxetin was predominant in exudates (but not in roots) of Fe-deficient *A. thaliana* plants grown at pH 7.5. Also, fraxetin was able to mobilize efficiently Fe from a Fe(III)-oxide at pH 5.5 and pH 7.5. On the other hand, non-catechol coumarins were much less efficient in mobilizing Fe and were present in much lower concentrations, making unlikely that they could play a role in Fe mobilization. The structural features of the array of coumarin type-compounds produced suggest some can mobilize Fe from the soil and others can be more efficient as allelochemicals.

Funding statement

Work supported by the Spanish Ministry of Economy and Competitiveness (MINECO) (grant AGL2013-42175-R, co-financed with FEDER) and the Aragón Government (group A03). PS-T and AL-V were supported by MINECO-FPI contracts.

Ethics statements

(Authors are required to state the ethical considerations of their study in the manuscript, including for cases where the study was exempt from ethical approval procedures)

Does the study presented in the manuscript involve human or animal subjects: No

1 **Accumulation and Secretion of Coumarinolignans and other**
2 **Coumarins in *Arabidopsis thaliana* Roots in Response to Iron**
3 **Deficiency at High pH**

4 **Patricia Sisó-Terraza¹†, Adrián Luis-Villarroya¹†, Pierre Fourcroy², Jean-François**
5 **Briat², Anunciación Abadía¹, Frédéric Gaymard², Javier Abadía¹, Ana Álvarez-**
6 **Fernández¹***

7 ¹Department of Plant Nutrition, Aula Dei Experimental Station, Consejo Superior de
8 Investigaciones Científicas, Zaragoza, Spain

9 ²Biochimie et Physiologie Moléculaire des Plantes, Centre National de la Recherche
10 Scientifique, Institut National de la Recherche Agronomique, Université Montpellier,
11 Montpellier, France

12 † These authors contributed equally to this work.

13 ***Correspondence:**

14 Ana Álvarez Fernández
15 Plant Nutrition Department
16 Aula Dei Experimental Station (CSIC)
17 P.O. Box 13034, E-50080, Zaragoza, Spain
18 Phone: +34976716064; FAX: +34976716145; e-mail: ana.alvarez@eead.csic.es
19

20 **Running title: Coumarins in Fe-deficient Arabidopsis Plants**

21 **Keywords: Arabidopsis, cleomiscosin, coumarin, fraxetin, iron nutrition, mass**
22 **spectrometry, root secretion**

23 Number of words: 10903

24 Number of figures: 8

25 Number of tables: 3

26

27 **Abstract**

28 Root secretion of coumarin-phenolic type compounds has been recently shown to be related
29 to *Arabidopsis thaliana* tolerance to Fe deficiency at high pH. These studies revealed the
30 identity of a few simple coumarins occurring in roots and exudates of Fe-deficient *A. thaliana*
31 plants, and left open the possible existence of other unknown phenolics. We used HPLC-UV-
32 VIS-ESI-MS(TOF), HPLC/ESI-MSn(ion trap) and HPLC-ESI-MS-MS(Q-TOF) to
33 characterize (identify and quantify) phenolic-type compounds accumulated in roots or
34 secreted into the nutrient solution of *A. thaliana* plants in response to Fe deficiency. Plants
35 grown with or without Fe and using nutrient solutions buffered at pH 5.5 or 7.5 enabled to
36 identify an array of phenolics. These include several coumarinolignans not previously
37 reported in *A. thaliana* (cleomiscosins A, B, C and D and the 5'-hydroxycleomiscosins A
38 and/or B), as well as some coumarin precursors (ferulic acid and coniferyl and sinapyl
39 aldehydes), and previously reported catechol (fraxetin) and non-catechol coumarins
40 (scopoletin, isofraxidin and fraxinol), some of them in hexoside forms not previously
41 characterized. The production and secretion of phenolics were more intense when the plant
42 accessibility to Fe was diminished and the plant Fe status deteriorated, as it occurs when
43 plants are grown in the absence of Fe at pH 7.5. Aglycones and hexosides of the four
44 coumarins were abundant in roots, whereas only the aglycone forms could be quantified in the
45 nutrient solution. A comprehensive quantification of coumarins, first carried out in this study,
46 revealed that the catechol coumarin fraxetin was predominant in exudates (but not in roots) of
47 Fe-deficient *A. thaliana* plants grown at pH 7.5. Also, fraxetin was able to mobilize efficiently
48 Fe from a Fe(III)-oxide at pH 5.5 and pH 7.5. On the other hand, non-catechol coumarins
49 were much less efficient in mobilizing Fe and were present in much lower concentrations,
50 making unlikely that they could play a role in Fe mobilization. The structural features of the
51 array of coumarin type-compounds produced suggest some can mobilize Fe from the soil and
52 others can be more efficient as allelochemicals.

53

54 1 Introduction

55 Iron (Fe) is required for many crucial biological processes, and is therefore essential for all
56 living organisms. A sufficient supply of Fe is necessary for optimal plant productivity and
57 agricultural produce quality (Briat et al., 2015). Iron is the fourth most abundant element in
58 the earth's crust, but its availability for plants is influenced by pH and redox potential, as well
59 as by the concentration of water-soluble Fe-complexes and the solubility of Fe(III)-oxides and
60 oxyhydroxides (Lindsay 1995). In calcareous soils, which cover more than 30% of the earth
61 surface, the high soil pH and low soil organic matter content lead to Fe concentrations in the
62 bulk soil solution far below those required for the optimal growth of plants and microbes (10^{-4} - 10^{-9}
63 and 10^{-5} - 10^{-7} M, respectively; Guerinot and Ying 1994). Since plants and microbiota
64 have evolved in soils poor in available Fe, they have active mechanisms for Fe acquisition,
65 often relying on the synthesis and secretion of an array of chemicals that modify the
66 neighboring environment and reduce competition for Fe (Crumbly and Harrington 2009; Jin
67 et al., 2014; Mimmo et al., 2014; Aznar et al., 2015). Some of these chemicals are capable to
68 mine Fe from the soil *via* solubilization, chelation and reduction processes, whereas others
69 can serve as repellants and/or attractants that inhibit and/or promote the growth of
70 concomitant organisms.

71 In plants, two different Fe uptake mechanisms have been characterized (Kobayashi and
72 Nishizawa 2012). *Graminaceae* species use a chelation-type strategy (Strategy II) based on
73 the synthesis of phytosiderophores (PS), metal-chelating substances of the mugineic acid
74 family: PS are released by roots *via* specific transporters, mine Fe(III) from the soil by
75 forming Fe(III)-PS complexes, and then complexes are taken up by transporters of the Yellow
76 Stripe family. Non-graminaceous species such as *Arabidopsis thaliana* use a reduction-type
77 strategy (Strategy I), based on the reduction of rhizospheric Fe(III) by a Fe(III) chelate
78 reductase (FRO, ferric reduction oxidase) and the uptake of Fe(II) by root plasma membrane
79 transporters (IRT, iron-regulated transporter). Other items of the Strategy I toolbox are an
80 enhanced H^+ -ATPase activity, an increased development of root hairs and transfer cells and
81 the synthesis and secretion into the rhizosphere of a wide array of small molecules, including
82 flavins, phenolic compounds and carboxylates (Cesco et al., 2010; Mimmo et al., 2014).
83 Recent studies have unveiled direct roles in root Fe acquisition for flavin secretion in *Beta*
84 *vulgaris* (Sisó-Terraza et al., 2016) and phenolics secretion in *Trifolium pratense* (Jin et al.,
85 2006, 2007) and *A. thaliana* (Rodríguez-Celma et al., 2013; Fourcroy et al., 2014, 2016;
86 Schmid et al., 2014; Schmidt et al., 2014).

87 The phenolic compounds category, including *ca.* 10,000 individual compounds in plants
88 (Croteau et al., 2000), has been long considered to be one of the major components of the
89 cocktail of small molecules secreted by roots of Fe-deficient plants (Cesco et al., 2010). In
90 particular, the coumarin compounds class (O-containing heterocycles with a benzopyrone
91 backbone; Figure 1a), which includes at least 1,300 compounds in plants (Borges et al., 2005)
92 has been the focus of recent studies with *A. thaliana*. Upon Fe deficiency, there is a
93 transcriptional up-regulation in roots both of the central phenylpropanoid pathway (from
94 phenylalanine ammonia lyase, one of the upstream enzymes in the pathway, to the
95 coumarate:CoA ligases 4CL1 and 4CL2 that mediate its last step) and of a crucial step of a
96 phenylpropanoid biosynthetic branch, the 2-oxoglutarate-dependent dioxygenase enzyme
97 feruloyl-CoA 6'-hydroxylase1 (F6'H1) (García et al., 2010; Yang et al., 2010; Lan et al.,
98 2011; Rodríguez-Celma et al., 2013; Fourcroy et al., 2014; Schmid et al., 2014; Schmidt et
99 al., 2014), which is responsible for the synthesis of the highly fluorescent coumarin scopoletin
100 (Kai et al., 2008). Up to now, a total of five coumarins, esculetin, fraxetin, scopoletin,

101 isofraxidin and an isofraxidin isomer have been described in Fe-deficient *A. thaliana* roots in
102 both glycoside and aglycone forms (Figure 1a and Supplementary Table S1; Fourcroy et al.,
103 2014; Schmid et al., 2014; Schmidt et al., 2014).

104 Root exudates from Fe-deficient *A. thaliana* plants contain the same coumarins that are
105 found in root extracts, with the aglycone forms being more prevalent (Supplementary Table
106 S1; Fourcroy et al., 2014; Schmid et al., 2014; Schmidt et al., 2014). These exudates have
107 been shown to solubilize 17-fold more Fe from an Fe(III)-oxide (at pH 7.2) when compared to
108 exudates from Fe-sufficient plants, and this was ascribed to the formation of Fe(III)-catechol
109 complexes (Schmid et al., 2014). It is noteworthy that the catechol moiety in two of the five
110 coumarins found to increase with Fe deficiency (esculetin and fraxetin) confers affinity for
111 Fe(III) at high pH and therefore capability for Fe(III) chelation in alkaline soils. In the
112 remaining three coumarins found so far (scopoletin, isofraxidin and its isomer), the catechol
113 moiety is capped *via* hydroxyl (-OH) group methylation (Figure 1a), whereas in the glycoside
114 forms of esculetin (esculetin 6-O-glucoside, known as esculin) and fraxetin (fraxetin 8-O-
115 glucoside, known as fraxin) the catechol is capped *via* hydroxyl group glycosylation (Figure
116 1a). When coumarin synthesis is impaired, as in the *A. thaliana f6'h1* mutant, plants are
117 unable to take up Fe from insoluble Fe sources at high pH (Rodríguez-Celma et al., 2013;
118 Schmid et al., 2014; Schmidt et al., 2014), root exudates are unable to solubilize Fe from
119 insoluble Fe sources, and supplementation of the agarose growth media with scopoletin,
120 esculetin or esculin restores the Fe-sufficient phenotype (Schmid et al., 2014). However, in *in*
121 *vitro* tests only esculetin (with a catechol moiety), was found to mobilize Fe(III) from an
122 Fe(III) oxide source at high pH (Schmid et al., 2014).

123 The secretion of coumarins by Fe-deficient roots involves an ABC (ATP-binding cassette)
124 transporter, ABCG37/PDR9, which is strongly over-expressed in plants grown in media
125 deprived of Fe (Yang et al., 2010; Fourcroy et al., 2014, 2016) or containing insoluble Fe(III)
126 at high pH (Rodríguez-Celma et al., 2013). The export of scopoletin, fraxetin, isofraxidin and
127 an isofraxidin isomer was greatly impaired in the mutant *abcg37* (Fourcroy et al., 2014),
128 which, as it occurs with *f6'h1*, is inefficient in taking up Fe from insoluble Fe(III) at pH 7.0
129 (Rodríguez-Celma et al., 2013). The root secretion of fluorescent phenolic compounds in *A.*
130 *thaliana* also requires the Fe deficiency-inducible β -glucosidase BGLU42 (Zamioudis et al.,
131 2014). On the other hand, the IRT1/FRO2 high-affinity root Fe uptake system is necessary for
132 the plant to take up Fe once mobilized, since *irt1* and *fro2* plants grown with unavailable Fe
133 and in absence of phenolics develop chlorosis (Fourcroy et al., 2016). The co-regulation of
134 *ABCG37* and coumarin synthesis genes with *FIT*, *IRT1*, *FRO2* and *AHA2* (Rodríguez-Celma
135 et al., 2013) as well as the requirement of *FIT* for *F6'H1* up-regulation upon Fe deficiency
136 (Schmid et al., 2014) support that all these components act in a coordinated mode.

137 Limitations inherent to the analytical procedures used and/or difficulties in compound
138 structure elucidation have prevented the full characterization of the changes in coumarin
139 composition promoted by Fe deficiency. First, HPLC coupled to fluorescence detection and
140 mass spectrometry (MS and MSⁿ) identification was used, therefore focusing only on
141 fluorescent coumarin compounds changing in response to Fe deficiency (Fourcroy et al.,
142 2014); a similar approach was taken later on by Schmid et al., (2014). In a second approach,
143 the use of full chromatographic MS profiles permitted the detection of dozens of compounds
144 changing with Fe deficiency, but only the same coumarins already found with the
145 fluorescence detection approach could be identified (Schmidt et al., 2014).

146 The aim of this study was to gain insight into the phenolic composition of *A. thaliana* root
147 exudates in response to Fe deficiency, a necessary step for a thorough understanding of the

148 function of phenolics in plant Fe acquisition. Root extracts and exudates from Fe-sufficient
149 and Fe-deficient *A. thaliana* plants grown at pH 5.5 and 7.5 have been analyzed by HPLC
150 coupled to five different detectors: fluorescence, photodiode array, MS-time of flight (TOF),
151 MS-ion trap and MS-MS tandem quadrupole (Q)-TOF, and identification and quantification
152 of phenolics was carried out in roots and exudates. Up to now, quantification of coumarins in
153 roots and exudates from Fe-deficient *A. thaliana* plants had been done only for the two
154 fluorescent compounds esculetin and scopoletin (Schmid et al., 2014). We report herein the
155 identification and quantification of coumarinolignans, coumarin precursors and additional
156 coumarin glycosides, among an array of phenolics accumulated and/or secreted by *A. thaliana*
157 roots in response to Fe deficiency. The root accumulation and secretion of coumarins and
158 coumarinolignans was much higher in plants grown at pH 7.5 than those grown at pH 5.5, and
159 the catechol coumarin fraxetin was predominant in nutrient solutions but not in root extracts.
160 These findings demonstrate the inherent chemical complexity involved in the survival of *A.*
161 *thaliana* in conditions of high competition for Fe, and give clues for the possible roles of
162 some of the phenolic compounds found.

163 **2 Materials and Methods**

164 **2.1 Plant Culture and Experimental Design**

165 *Arabidopsis thaliana* (L.) Heynh (ecotype Col0) seeds were germinated, pre-grown and
166 grown as indicated in Fourcroy et al. (2014) with several modifications. Germination and
167 plant growth took place in a controlled environment chamber (Fitoclima 10000 EHHF,
168 Aralab, Albarraque, Portugal), at 21°C, 70% relative humidity and a photosynthetic photon
169 flux density of 220 $\mu\text{mol m}^{-2} \text{s}^{-1}$ photosynthetic active radiation with a photoperiod of 8 h
170 light/16 h dark. Seeds were sown in 0.2 ml tubes containing 0.6% agar prepared in nutrient
171 solution 1/4 Hoagland, pH 5.5. Iron was added as 45 μM Fe(III)-EDTA. After 10 d in the
172 growth chamber, the bottom of the tubes containing seedlings was cut off and the tubes were
173 placed in opaque 300-ml plastic boxes (pipette tip racks; Starlab, Hamburg, Germany),
174 containing aerated nutrient solution 1/2 Hoagland, pH 5.5, supplemented with 20 μM Fe(III)-
175 EDTA. Plants were grown for 11 d and nutrient solutions were renewed weekly. After that,
176 plants (12 plants per rack) were grown for 14 d in nutrient solution 1/2 Hoagland with 0 or 20
177 μM Fe(III)-ethylendiaminedi(*o*-hydroxyphenylacetate) (Fe(III)-EDDHA; Sequestrene,
178 Syngenta, Madrid, Spain). Solutions were buffered at pH 5.5 (with 20 mM MES) or at 7.5
179 (with 5 mM HEPES) to maintain a stable pH during the whole treatment period. Nutrient
180 solutions were renewed weekly. Two batches of plants were grown and analyzed. Pots
181 without plants, containing only aerated nutrient solution (with and without Fe) were also
182 placed in the growth chamber and the nutrient solutions sampled as in pots containing plants;
183 these samples were later used as blanks for root exudate analyses.

184 Roots were sampled 3 d after the onset of Fe deficiency treatment, immediately frozen in
185 liquid N₂, and stored at -80 °C for RNA extraction. Nutrient solutions were sampled at days 7
186 and 14 after the onset of Fe deficiency treatment, and immediately stored at -20 °C until
187 extraction of phenolic compounds. Shoots and roots were sampled separately at the end of the
188 experimental period. Leaf disks (0.1 cm²) were taken from young leaves and stored at -20°C
189 for photosynthetic pigment analysis. Roots were washed with tap water and then with type I
190 water, dried with filter paper, and then frozen immediately (in aliquots of approximately 300
191 mg) in liquid N₂ and stored at -80 °C until extraction of phenolic compounds. Roots and
192 shoots from 12 plants per treatment and replication were processed for mineral analysis as in
193 Fourcroy et al. (2014).

194

195 2.2 Photosynthetic Pigment Composition

196 Leaf pigments were extracted with acetone in the presence of Na ascorbate and stored as
197 described previously (Abadía and Abadía, 1993). Pigment extracts were thawed on ice,
198 filtered through a 0.45 µm filter and analyzed by HPLC-UV/visible as indicated in Larbi et al.
199 (2004), using a HPLC apparatus (600 pump, Waters, Mildford, MA, USA) fitted with a
200 photodiode array detector (996 PDA, Waters). Pigments determined were total chlorophyll
201 (*Chl a* and *Chl b*), neoxanthin, violaxanthin, taraxanthin, antheraxanthin, lutein, zeaxanthin
202 and carotenoids. All chemicals used were HPLC quality.

203 2.3 Mineral Analysis

204 Plant tissues were ground and digested as indicated in Fourcroy et al. (2014). Iron, Mn, Cu
205 and Zn were determined by flame atomic absorption spectrometry using a SOLAAR 969
206 apparatus (Thermo, Cambridge, UK).

207 2.4 Extraction of Phenolic Compounds from Roots and Nutrient Solutions

208 Phenolic compounds were extracted from roots and nutrient solutions as described in
209 Fourcroy et al. (2014), with some modifications. First, extraction was carried out without
210 adding internal standards (IS) to identify relevant compounds, including those increasing (or
211 appearing) with Fe deficiency. This extract was also used to check for the presence of the
212 compounds used as IS and other endogenous isobaric compounds that may co-elute with
213 them, since in both cases there will be analytical interferences in the quantification process.
214 The extraction was then carried out adding the following three IS compounds: artemicapin C
215 (Figure 1d), a methylenedioxy-coumarin, for quantification of the coumarins scopoletin,
216 fraxetin, isofraxidin and fraxinol; esculin (Figure 1a), the glucoside form of the coumarin
217 esculetin, for quantification of coumarin glycosides; and the lignan matairesinol (Figure 1d),
218 for quantification of coumarinolignans.

219 Frozen roots (*ca.* 100 mg) were ground in liquid N₂ using a Retsch M301 ball mill (Restch,
220 Düsseldorf, Germany) for 3 min and then phenolic compounds were extracted with 1 ml of
221 100% LC-MS grade methanol, either alone or supplemented with 20 µl of a IS solution (37.5
222 µM artemicapin C, 50 µM esculin and 37.5 µM matairesinol) by homogenization in the same
223 mill for 5 min. The supernatant was recovered by centrifugation (12,000 xg at 4°C and 5
224 min), and stored at -20°C. The pellet was re-suspended in 1 ml of 100% methanol,
225 homogenized again for 5 min and the supernatant recovered. The two supernatant fractions
226 were pooled, vacuum dried in a SpeedVac (SPD111V, Thermo-Savant, Thermo Fisher
227 Scientific, Waltham, Massachusetts, MA, USA) and dissolved with 250 µl of a solution
228 containing 15% methanol and 0.1% formic acid. Extracts were filtered through poly-
229 vinylidene fluoride (PVDF) 0.45 µm ultrafree-MC centrifugal filter devices (Millipore) and
230 stored at -80°C until analysis.

231 Phenolic compounds in the nutrient solutions (300 ml of solution used for the growth of 12
232 plants) were retained in a SepPack C₁₈ cartridge (Waters), eluted from the cartridge with 2 ml
233 of 100% LC-MS grade methanol, and the eluates stored at -80°C. Samples were thawed and a
234 400 µl aliquot was dried under vacuum (SpeedVac) alone or supplemented with 10 µl of a IS
235 solution (80 µM artemicapin C and 150 µM matairesinol). Dried samples were dissolved in
236 15% methanol and 0.1% formic acid to a final volume of 100 µl, and then analyzed by HPLC-
237 MS. No determinations could be made in nutrient solutions of Fe-sufficient plants due to the
238 presence of Fe(III)-EDDHA, that causes the overloading of C₁₈ materials.

239

240 2.5 Extraction of Cleomiscosins from *Cleome viscosa* Seeds

241 Cleomiscosins were extracted from *Cleome viscosa* seeds (B & T World Seeds, Paguignan,
242 France) as described by Chattopadhyay et al. (2008). Seeds were ground using a Retsch M400
243 ball mill and 25 g of the powder was defatted by homogenization with 50 ml petroleum ether
244 at 25°C for 48 h. The defatting procedure was repeated three times. The solid residue was
245 extracted with 50 ml methanol for 48 h at 25°C, and the extraction was repeated three times.
246 The methanolic extracts were pooled, dried with a rotavapor device and the residue dissolved
247 in 15% methanol and 0.1% formic acid.

248 2.6 Phenolic Compounds Analysis by HPLC-Fluorescence and HPLC-UV/VIS-ESI- 249 MS(TOF)

250 HPLC-fluorescence analyses were carried out using a binary HPLC pump (Waters 125)
251 coupled to a scanning fluorescence detector (Waters 474) as in Fourcroy et al., (2014).
252 Separations were performed using an analytical HPLC column (Symmetry® C₁₈, 15 cm x 2.1
253 mm i.d., 5 µm spherical particle size, Waters) protected by a guard column (Symmetry® C₁₈,
254 10 mm x 2.1 mm i.d., 3.5 µm spherical particle size, Waters) and a gradient mobile phase
255 built with 0.1% (v/v) formic acid in water and 0.1% (v/v) formic acid in methanol (Elution
256 program 1; Supplementary Table S2). The flow rate and injection volume were 0.2 ml min⁻¹
257 and 20 µl, respectively. Phenolic compounds were detected using λ_{exc} 365 and λ_{em} 460 nm.

258 HPLC-UV/VIS-ESI-MS(TOF) analysis was carried out with an Alliance 2795 HPLC
259 system (Waters) coupled to a UV/VIS (Waters PDA 2996) detector and a time-of-flight mass
260 spectrometer [MS(TOF); MicrOTOF, Bruker Daltonics, Bremen, Germany] equipped with an
261 electrospray (ESI) source. Two HPLC protocols were used, the one described above and a
262 second one with a different elution program (Elution program 2; Supplementary Table S2)
263 designed to improve the separation of the phenolic compounds of interest. The ESI-MS(TOF)
264 operating conditions and software used were as described in Fourcroy et al., (2014). Mass
265 spectra were acquired in positive and negative ion mode in the range of 50-1000 mass-to-
266 charge ratio (*m/z*) units. The mass axis was calibrated externally and internally using Li-
267 formate adducts [10 mM LiOH, 0.2% (v/v) formic acid and 50% (v/v) 2-propanol]. The
268 internal mass axis calibration was carried out by introducing the calibration solution with a
269 divert valve at the first and last three minutes of each HPLC run. Molecular formulae were
270 assigned based on exact molecular mass with errors < 5 ppm (Bristow, 2006). Phenolic
271 standards used are shown in Supplementary Table S3. Concentrations of phenolic compounds
272 were quantified using external calibration with internal standardization with the exception of
273 ferulic acid hexoside and the cleomiscosins. Ferulic acid hexoside was quantified as fraxin
274 because there is no commercially available authenticated standard. The levels of the
275 cleomiscosins are expressed in peak area ratio, relative to the lignan matairesinol used as
276 internal standard. For quantification, analytes and IS peak areas were obtained from
277 chromatograms extracted at the *m/z* (± 0.02) ratios corresponding to [M+H]⁺ ions, with the
278 exception of glycosides, where the *m/z* ratios corresponding to [M-hexose+H]⁺ ions were
279 used.

280 2.7 Phenolic Compounds Analysis by HPLC-ESI/MS(Q-TOF) and by HPLC/ESI 281 MS/MS(ion trap)

282 Phenolic compounds were also analyzed by HPLC/ESI-MS(Q-TOF) using a 1100 HPLC
283 system (Agilent Technologies) coupled to a quadrupole time-of-flight mass spectrometer (Q-
284 TOF; MicroTOF-Q, Bruker Daltonics) equipped with an ESI source. The HPLC conditions

285 were described in Fourcroy et al., (2014) (see above and Supplementary Table S2). The ESI-
286 MS(Q-TOF) operating conditions were optimized by direct injection of 50 μM solutions of
287 phenolic compound standards at a flow rate of 250 $\mu\text{l h}^{-1}$. Mass spectra (50-1000 m/z range)
288 were acquired in positive ion mode, with capillary and endplate offset voltages of 4.5 kV and
289 -0.5 kV, respectively, and a collision cell energy of 100-2000 eV. The nebulizer (N_2) gas
290 pressure, drying gas (N_2) flow rate and drying gas temperature were 1.0 bar, 4.0 L min^{-1} and
291 200 $^\circ\text{C}$, respectively. The mass axis was calibrated externally and internally as indicated
292 above for the HPLC-ESI-MS(TOF) analysis. Molecular formulae for the product ions were
293 assigned based on exact molecular mass with errors < 5 ppm (Bristow 2006).

294 HPLC-ESI-MS/MS (ion trap) analysis was carried out with an Alliance 2795 HPLC
295 system (Waters) coupled to an ion-trap mass spectrometer (HCT Ultra, BrukerDaltonics)
296 equipped with an ESI source. The HPLC conditions were as described in Fourcroy et al
297 (2014) and Supplementary Table S2 (Elution program 2). ESI-ion trap-MS analysis was
298 carried out in positive ion mode, the MS spectra were acquired in the standard mass range
299 mode and the mass axis was externally calibrated with a tuning mix (Agilent). The HCT Ultra
300 was operated with settings shown in Supplementary Table S4. The protonated ions of interest
301 $[\text{M}+\text{H}]^+$ were subjected to collision induced dissociation (CID; using the He background gas
302 present in the trap for 40 ms) to produce a first set of fragment ions, MS/MS or MS^2 .
303 Subsequently, some of the fragment ions were isolated and fragmented to give the next set of
304 fragment ions, MS^3 and so on. For each precursor ion, fragmentation steps were optimized by
305 visualizing fragment intensity changes.

306 2.8 RNA Extraction and Quantitative RT-PCR Analysis

307 Total RNA was extracted from roots using the RNeasy Plant Mini Kit (Quiagen). One
308 microgram RNA was treated with RQ1 DNase (Promega) before use for reverse transcription
309 (Goscript reverse transcriptase; Promega) with oligo (dT)18 and 0.4 mM dNTPs (Promega).
310 The cDNAs were diluted twice with water, and 1 μl of each cDNA sample was assayed by
311 qRT-PCR in a LightCycler 480 (Roche Applied Science) using Lightcycler 480 SYBR Green
312 master I (Roche Applied Science). Expression levels were calculated relative to the
313 housekeeping gene PP2 (At1g13320) using the $\Delta\Delta\text{CT}$ method to determine the relative
314 transcript level. The primers used for qRT-PCR were those described in Fourcroy et al. (2014)
315 and indicated in Supplementary Table S5.

316 2.9 Dissolution of Fe(III)oxide using coumarins

317 Ten milligrams of poorly crystalline Fe(III)-oxide was incubated (in the dark at 25 $^\circ\text{C}$) for 6 h
318 with 1.5 ml of an assay solution containing appropriated concentrations (in the range of 0 to
319 100 μM) of different coumarins (fraxin, fraxetin, scopoletin and isofraxidin) and 600 μM of
320 bathophenanthrolinedisulphonate (BPDS) -as Fe(II) trapping agent- and buffered at pH 5.5
321 (with 5 mM MES-KOH) or pH 7.5 (with 5 mM HEPES-KOH). Afterwards, the assay
322 medium was filtered through PVDF 0.22 μm centrifugal filters (Millipore) at 10,000 g for 1
323 min. Absorbance was measured at 535 nm in the filtrates and then the Fe(II) concentration
324 determined as Fe(II)-BPDS₃ using an extinction coefficient of 22.14 $\text{mM}^{-1} \text{cm}^{-1}$. The filtrates
325 were also measured for total Fe by Inductively Coupled Plasma Mass Spectrometry (ICP-MS,
326 Agilent 7500ce, Santa Clara, CA, USA) after diluting a 50 μl aliquot with 65% ultrapure
327 HNO_3 (TraceSELECT Ultra, Sigma-Aldrich).

328 2.10 Statistical Analyses

329 Statistical analysis was carried out with SPSS for PC (v.23.0, IBM, Armonk, NY, USA),
330 using ANOVA or nonparametric tests ($P \leq 0.05$), and a Levene test for checking homogeneity
331 of variances. Post hoc multiple comparisons of means corresponding to each one the four
332 different treatments were carried out ($P \leq 0.05$) using Duncan test when variances were equal
333 and Games–Howell’s test when variances were unequal.

334 **3 Results**

335 **3.1 Changes in Leaf Photosynthetic Pigment Concentrations, Fe Contents and** 336 **Biomass with Fe Deficiency and High pH**

337 *Arabidopsis thaliana* plants grown for 14 d in zero-Fe nutrient solution, buffered at either pH
338 5.5 or pH 7.5, had visible symptoms of leaf chlorosis (Figure 2a). The Chlorophyll (*Chl*)
339 concentration in young leaves decreased by 56% in response to Fe deficiency, but was
340 unaffected by the nutrient solution pH (Figure 2b). The concentrations of other photosynthetic
341 pigments (neoxanthin, violaxanthin, lutein and β -carotene) in young leaves also decreased
342 upon Fe deficiency (in the range of 48-60%) and were unaffected by the plant growth pH
343 (Supplementary Table S6).

344 Iron deficiency decreased shoot biomass by 32% only when plants were grown at pH 7.5,
345 whereas root biomass did not change significantly (Figure 2c). Shoot Fe content decreased
346 significantly with Fe deficiency only in plants grown at pH 5.5 (by 61%; Figure 2c), whereas
347 root Fe content was markedly decreased by 92% in plants grown at both pH values (Figure
348 2c). Iron deficiency also affected the contents of other micronutrients in plants, and this
349 occurred mainly in shoots (Supplementary Table S7). The largest change found was a 6-fold
350 increase over the control value in the shoot Cu content of plants grown at pH 5.5.

351 **3.2 Changes in the Expression of Genes Involved in Fe Root Uptake and the** 352 **Phenylpropanoid Pathway with Fe Deficiency and High pH**

353 The transcript levels of *IRT1*, *FRO2*, *ABCG37*, *F6’HI*, the caffeic acid/5-hydroxyferulic acid
354 O-methyltransferase (*COMT*) and the trans-caffeoyl-CoA 3-O-methyltransferase (*CCoAMT*)
355 were assessed by quantitative RT-PCR in control (Fe-sufficient) and Fe-deficient roots from
356 both plants grown at pH 5.5 or at pH 7.5 three days after treatment onset (Figure 2d). Under
357 high Fe supply, the only pH effect observed was for *FRO2*, whose transcript abundance was
358 12-fold higher in plants grown at pH 7.5 than in those grown at pH 5.5. Under Fe deficiency
359 conditions, *IRT1* and *FRO2* gene expression increased in plants grown both at pH 5.5 and pH
360 7.5; the increases were 9-fold for *IRT1* and 15-fold for *FRO2* in plants grown at pH 5.5, and
361 20-fold for *IRT1* and 5-fold for *FRO2* in plants grown at pH 7.5. Other genes studied,
362 *ABCG37* and *F6’HI*, also showed increases in their expression in response to Fe deficiency
363 when compared to the Fe-sufficient controls, although they were smaller than those observed
364 for *IRT1* and *FRO2*. The increases in *ABCG37* gene expression were 2- (although this change
365 was not statistically significant) and 4-fold in plants grown at pH 5.5 and pH 7.5, respectively,
366 whereas those of *F6’HI* were 4- and 8-fold in plants grown at pH 5.5 and pH 7.5. On the
367 other hand, *COMT* and *CCoAMT* gene expression in roots was only increased by Fe
368 deficiency at pH 7.5 (2-fold).

369 **3.3 Arabidopsis Roots Accumulate and Secrete an Array of Fluorescent and Non-** 370 **Fluorescent Phenolic-Type Compounds with Fe Deficiency and High pH**

371 Methanolic extracts of roots of *A. thaliana* plants and their nutrient solutions were analyzed
372 using the reverse phase C₁₈ HPLC-based method used in Fourcroy et al. (2014) (Elution

373 program 1), using both UV/VIS detection in the range 200-600 nm and fluorescence detection
374 at λ_{exc} 365 and λ_{em} 460 nm (only the latter was used in the original study). Fluorescence alone
375 cannot detect all phenolic compounds, since many of them emit little or no fluorescence.
376 However, all phenolic compounds absorb light in the UV region; coumarins, their derivatives
377 and precursors (e.g., ferulic and other cinnamic acids) have absorption maxima in the range
378 290-330 nm.

379 This is illustrated by the absorbance chromatograms of *A. thaliana* root extracts and
380 growth media at 320 nm, which show many additional peaks to those found in fluorescence
381 chromatograms obtained with the same samples (Figure 3). Each of the peaks in the
382 chromatogram may contain one or more compounds (either fluorescent and/or non-
383 fluorescent; see sections below for identification). In the control root extracts, fluorescence
384 chromatograms showed only two peaks at approximately 10 and 15 min, whereas the
385 absorbance chromatograms show several small peaks at two retention time (RT) ranges, 9-16
386 and 19-24 min, as well as a large peak at approximately 18 min (Figure 3). In the root extracts
387 from Fe-deficient plants, increases were found in fluorescence in the area of the 15 min peak
388 and in absorbance in the 18 min peak. In the control nutrient solution, the fluorescence
389 chromatogram showed peaks at 10, 15 and 19 min, whereas the absorbance chromatogram
390 showed peaks at 18 min and 19 min (Figure 3). Iron deficiency caused large increases in the
391 areas of all these peaks, with further absorbance ones appearing at 13, 14, 15, 16 and 17 min.
392 This shows that Fe deficiency induces the synthesis, root accumulation and secretion to the
393 growth media not only of fluorescent coumarins, as described by Fourcroy et al. (2014) and
394 Schmid et al. (2014), but also of a number of previously unreported non-fluorescent phenolic
395 compounds.

396 **3.4 Identification of the Non-Fluorescent Compounds Induced by Fe Deficiency as** 397 **Coumarins, Coumarin Precursors and Coumarinolignans**

398 To identify the compounds found in the *A. thaliana* root extracts and growth media, samples
399 were analyzed using four different HPLC-UV-VIS-ESI-MS(TOF) protocols, including two
400 Elution programs (1 and 2; Supplementary Table S2) and two electrospray (ESI) ionization
401 modes (positive and negative). The newly designed Elution program 2 led to a better
402 separation of phenolic compounds than that obtained with the original Elution program 1 used
403 in Fourcroy et al. (2014). With the new elution program, RTs for a selected set of phenolics
404 standards ranged from 8.4 (for esculin, the glucoside form of the coumarin esculetin) to 51.7
405 min (for the flavone apigenin) (Supplementary Figures S1 and S2). These HPLC-ESI-
406 MS(TOF) analyses provided highly accurate (error below 5 ppm) measurements of the mass-
407 to-charge (m/z) ratio of the detected ions, therefore allowing for accurate elemental formulae
408 assignments (Bristow 2006).

409 Raw MS(TOF) datasets (time, m/z and ion intensity) from the root extracts and nutrient
410 solutions from Fe-deficient and Fe-sufficient plants were first analyzed with the DISSECT
411 algorithm (Data Analysis 4.0; Bruker) to obtain mass spectral features attributable to
412 individual compounds. From a total of approximately 180 possible mass spectral features
413 analyzed per run and sample, only 18 complied with the following two requirements: i)
414 occurring at chromatographic RTs where absorbance at 320 nm was observed, and ii)
415 showing peak area increases (or appearing) with Fe-deficiency. Then, associated ions coming
416 from adducts (with salts or solvents), dimers and trimers were discarded (with some
417 exceptions, see below), and the ion chromatograms of all major remaining ions (including
418 non-fragmented ones as well as fragment ions produced in the ESI source) were extracted
419 with a precision of $\pm 0.02 m/z$. From these, we selected major ions showing large changes in

420 peak areas in response to Fe deficiency, without considering fragments and minor ions. The
421 localization in the chromatograms of the 18 selected compounds is depicted in Figure 3, and
422 the RT, exact m/z and assigned elemental formulae are shown in Table 1. These 18
423 compounds were never detected in nutrient solutions of pots without plants, and include some
424 coumarins already known to occur and others not previously reported, as explained in detail
425 below.

426 **3.4.1 Coumarins and Related Compounds Previously Reported in *A. thaliana* upon Fe-** 427 **Deficiency**

428 As expected, some compounds (five out of 18) have RTs and m/z values matching with those
429 of coumarins previously found in roots and exudates from Fe-deficient *A. thaliana* plants
430 (Fourcroy et al., 2014, Schmid et al., 2014, Schmidt et al., 2014). These include compounds 1,
431 7-9 and 11 (Figure 3 and Table 1), and were assigned to scopoletin hexoside, fraxetin,
432 scopoletin, isofraxidin and fraxinol (an isofraxidin isomer), respectively (Supplementary
433 Table S1). These annotations were further confirmed using the RT and m/z values of
434 standards (Table 1 vs. Table 2). A sixth compound, 2, was assigned to ferulic acid hexoside
435 based on the presence of a major ion at m/z 195.0656 in its positive MS(TOF) spectrum,
436 which is consistent with the elemental formula of ferulic acid $[M+H]^+$ ion (Table 2) and with
437 the neutral loss of a hexosyl moiety (162.0528 Da, $C_6H_{10}O_5$) from the $[M+H]^+$ ion (with an
438 absolute error of 1.2 ppm). We could not confirm the identity using a ferulic acid hexoside
439 standard because to the best of our knowledge no such standard is commercially available.

440 The remaining 12 compounds were subjected to further MS-based analyses to obtain
441 structural information. First, low resolution HPLC-ESI-MS(ion trap) analyses were carried
442 out, including MS² and/or MS³ experiments with the $[M+H]^+$ or $[M-H]^-$ ions.

443 **3.4.2 Coumarins and Coumarin-Precursor Hexosides not Previously Reported in** 444 ***Arabidopsis* upon Fe-Deficiency**

445 Three of the compounds (10, 12 and 13) were identified as ferulic acid, coniferyl aldehyde
446 and sinapyl aldehyde (three phenylpropanoid precursors; Figure 1b), respectively, by
447 comparing the MS spectra of the analytes and those of standards: there was a good match of
448 the RT values and exact m/z ratios of the $[M+H]^+$ and $[M-H]^-$ ions (Tables 1 and 2) as well as
449 of the MS² spectra of the $[M+H]^+$ ions (Tables 2 and 3).

450 Four more compounds (3-6) were first confirmed to be hexoside-type compounds from the
451 RT, exact m/z values and MS² spectra of the $[M-H]^-$ ions. The RT values of these compounds
452 (12.3-14.9 min) were close to those of known coumarin glucosides (10.3 and 13.0 min for
453 scopolin and fraxin, respectively), and lower than those of coumarin aglycones (16.4-25.1 min
454 for fraxetin, scopoletin, isofraxidin and fraxinol), phenylpropanoids (e.g., 23.0 and 25.1 min
455 for ferulic acid and sinapyl aldehyde), and glycoside and aglycone forms of other phenolics
456 (e.g., 27-52 min for flavonoids, stilbenes and lignans) (Supplementary Figures S1 and S2).
457 Therefore, the RTs indicate that compounds 3-6 are likely to be polar (i.e., hexoside) forms of
458 coumarins and/or phenylpropanoids. Furthermore, in the MS(TOF) spectra, ions
459 (positive/negative) at m/z 179.0707/177.0544, 209.0450/207.0289, 223.0600/221.0447 and
460 209.0801/207.0648 for 3, 4, 5 and 6, respectively, were consistent with the loss of a hexosyl
461 moiety (162.05 Da) from their corresponding $[M+H]^+/[M-H]^-$ ions (see m/z values in Table
462 1). This was confirmed using the low resolution MS² spectra obtained with the ion trap: major
463 fragment ions (100% relative intensity at m/z 177, 207, 221 and 207 in the MS² spectra of 3-6,
464 respectively; Table 3) corresponded to the $[M-H]^-$ ions (m/z 339, 369, 383 and 369 for 3, 4, 5

465 and 6, respectively) after a mass loss of 162 Da. The same mass loss was also observed in the
466 MS² spectra of authenticated standards of the coumarin glucosides scopolin and fraxin
467 described above, with major ions at *m/z* 193/191 (scopolin) and 209/207 (fraxin),
468 corresponding with the *m/z* of their aglycones, scopoletin and fraxetin, respectively (Table 2).
469 The rest of ions in the MS² spectra of compounds 3-6, scopolin and fraxin showed
470 significantly lower relative intensities (<40%), indicating the hexosyl loss is favored.

471 The aglycon moieties of compounds 3-6 were identified taking advantage of having the
472 dehexosylated ions in the MS(TOF) spectra and also carrying out low resolution MS³
473 experiments on the ion trap. First, from the positive and negative MS(TOF) spectra, the *m/z*
474 values for dehexosylated ions (see above) of 3, 4, 5 and 6 were assigned to the elemental
475 formulae C₁₀H₁₀O₃, C₁₀H₈O₅, C₁₁H₁₀O₅ and C₁₁H₁₂O₄, respectively (with absolute errors < 4
476 ppm). Two of these elemental formulae, C₁₀H₁₀O₃ and C₁₁H₁₂O₄, were consistent with
477 coniferyl and sinapyl aldehydes, involved in coumarin synthesis (Kai et al., 2008) (Table 2),
478 whereas the other two, C₁₀H₈O₅ and C₁₁H₁₀O₅, were consistent with two coumarins already
479 identified in the samples (compounds 7 and 9, respectively) (Table 1). Finally, compounds 3-
480 6 were confirmed as the hexoside forms of coniferyl aldehyde, fraxetin, isofraxidin and
481 sinapyl aldehyde, respectively (Table 1) from the good fit between the MS³ ion trap spectra of
482 3-6 (339→177, 369→207, 383→221 and 369→207, respectively) (Table 3) and the MS²
483 spectra of the corresponding aglycone standards (Table 2).

484 3.4.3 Coumarinolignans: Newly Identified Compounds Synthesized in Response to Fe- 485 Deficiency

486 The last five compounds (14-18 in Table 1) are very hydrophobic, since they elute later (RTs
487 31-39 min) than compounds 1-13 (RTs 10-25 min), and have *m/z* values supporting elemental
488 formulae with a high number of C atoms (20-21 vs 10-17 for compounds 1-13). In fact, the
489 RTs of 14-18 are in line with those of phenolics bearing either C₁₅ (C₆-C₃-C₆; as in flavonoids
490 and stilbens) or C₁₈ (C₆-C₃-C₃-C₆; as in lignans) skeletons (27-52 min; Supplementary Figures
491 S1 and S2), whereas compounds 7-13 (coumarins and phenylpropanoids) share a C₉ (C₃-C₆)
492 skeleton and compounds 1-6 (hexose conjugates of 7-13) share a C₁₅ (C₃-C₆-C₆) skeleton
493 (Table 1).

494 The MS(TOF) spectra show that compounds 15-18 are two pairs of isomers, with
495 elemental formulae C₂₁H₂₀O₉ for 15-16 and C₂₀H₁₈O₈ for 17-18, with the difference between
496 formulae being consistent with a single methoxy (-OCH₃) group. The elemental formula of
497 compound 14, C₂₀H₁₈O₉, is consistent with the addition of both a hydroxyl (-OH) group to 17-
498 18 or the addition of a methyl (-CH₃) group to 15-16. The presence of these structural
499 differences are common among phenolics, since part of the phenylpropanoid biosynthesis
500 proceeds *via* a series of ring hydroxylations and O-methylations. The low resolution MS²
501 spectra from 14-18 (Figure 4a) indicate that these five compounds have highly related
502 chemical structures: i) the spectra of 15-16 show the same ions with only some differences in
503 their relative intensity, and the same was also observed for 17-18; ii) most of the ions in the
504 15-18 spectra were either common (*m/z* 263, 233, 209, 161) or consistent with common mass
505 losses from the [M+H]⁺ ion (e.g., *m/z* 367 and 337 in the 15-16 and 17-18 MS² spectra,
506 corresponding to a mass loss of 50 Da; Supplementary Table S8), and iii) the spectrum of 14
507 also has some of these features, including an ion at *m/z* 209 and a mass loss of 30 Da from the
508 [M+H]⁺ ion (Supplementary Table S8). When the MS² spectra of 14-18 were obtained on a
509 high resolution Q-TOF mass analyzer, which allows for an accurate mass determination of
510 fragment ions, all spectra showed a common fragment ion at *m/z* 209.0435, consistent with
511 the elemental formula C₁₀H₉O₅⁺ (with an error of -4.7 ppm) (Supplementary Figure S3) of the

512 dihydroxymethoxycoumarin fraxetin (compound 7). The presence of a fraxetin moiety in
513 compounds 14-18 was further confirmed by their MS³ spectra (403→209, 417→209,
514 417→209, 387→209 and 387→209 for 14, 15, 16, 17 and 18, respectively; Figure 4b), which
515 match perfectly with the fraxetin MS² spectrum.

516 Among the plant-derived fraxetin derivatives known so far (Begum et al., 2010; Zhang et
517 al., 2014), six coumarinolignans have elemental formulae consistent with those of compounds
518 14-18, including cleomiscosins A, B, C (also known as aquillochin) and D, first isolated and
519 identified in seeds of *Cleome viscosa* (a common weed of the *Capparidaceae* family), and 5'-
520 hydroxycleomosicosins A (also known as 5'-demethylaquillochin) and B, first isolated from
521 *Mallotus apelta* roots and *Eurycorymbus cavaleriei* twigs, respectively. Cleomiscosins C and
522 D (regioisomers -also called constitutional isomers- arising from the fusion of fraxetin and the
523 monolignol sinapyl alcohol through a dioxane bridge; Figure 1c) have a formula identical to
524 that of 15-16 (C₂₁H₂₀O₉), cleomiscosins A and B (regioisomers arising from the fusion of
525 fraxetin and the monolignol coniferyl alcohol through a dioxane bridge; Figure 1c) have a
526 formula identical to that of 17-18 (C₂₀H₁₈O₈), whereas 5'-hydroxycleomosicosins A and B
527 (regioisomers arising from the fusion of fraxetin and the monolignol hydroxyconiferyl
528 alcohol, Cheng and Chen 2000, Figure 1c), have a formula identical to that of compound 14
529 (C₂₀H₁₈O₉). The structural differences among these coumarinolignans -corresponding to the
530 monolignol moiety (Figure 1b)- are identical to those found among the elemental formulae of
531 14-18: i) a methoxy group differentiates coniferyl from sinapyl alcohols and the elemental
532 formula of 17-18 from that of 15-16; ii) a hydroxyl group differentiates hydroxyconiferyl
533 from coniferyl alcohols and the elemental formula of 14 from that of 17-18; and iii) a methyl
534 group differentiates hydroxyconiferyl and sinapyl alcohols and the formula of 14 from those
535 of 15-16.

536 To confirm the identification of 15-18 as cleomiscosins, we isolated coumarinolignans
537 from *C. viscosa* seeds. The seed isolate was analyzed by both HPLC-UV-VIS-ESI-MS(TOF)
538 and HPLC-ESI-MS/MS(ion trap) using Elution program 2 and positive ESI ionization. The
539 HPLC-ESI-MS(TOF) chromatogram for *m/z* 417.12 ± 0.02, corresponding to the
540 cleomiscosins C and D [M+H]⁺ ions, showed only two peaks, at 35.4 and 37.0 min, matching
541 with the RTs of 15 and 16 (Figure 4c and Table 1). Similarly, the HPLC-ESI-MS(TOF)
542 chromatogram for *m/z* 387.11±0.02, corresponding to the cleomiscosins A and B [M+H]⁺
543 ions, showed only two peaks, at 37.0 and 38.4 min, matching with the RTs of 17-18 (Figure
544 4c and Table 1). Peaks were assigned to cleomiscosin isomers according to the elution order
545 reported in the literature (Chattopadhyay et al., 2008; Kaur et al., 2010). These annotations
546 were confirmed by the full match between the MS² spectra of the cleomiscosins D, C, B and
547 A, and those of compounds 15, 16, 17 and 18, respectively (Figure 4c). Compound 14 eluted
548 at shorter times than the cleomiscosins (30.7 vs. 35.5-38.6 min), as expected from the
549 structural differences between 5'-hydroxycleomosicosins A and B and cleomiscosins (see
550 above). Furthermore, compound 14 shares elemental formula and the presence of a fraxetin
551 moiety with 5'-hydroxycleomosicosins A and B, and its MS² spectrum showed a loss of 18 Da
552 from the [M+H]⁺ ion (Figure 4b and Supplementary Table S8), which was previously
553 reported for 5'-hydroxycleomosicosin A (Cheng and Chen 2000) but does not occur in
554 cleomiscosins. Therefore, 14 was putatively annotated as 5'-hydroxycleomosicosin A and/or B
555 (Table 3).

556 3.5 Coumarin and Coumarinolignan Concentrations in Root Extracts

557 Quantification of phenolic compounds was carried out using the [M+H]⁺ and [M-
558 hexoside+H]⁺ signals in the HPLC-MS(TOF). Coumarins and their hexosides were quantified

559 using authenticated standards, whereas coumarinolignan concentrations were estimated using
560 peak/area ratios relative to that of the IS lignan matairesinol (Figure 1d), because of the lack
561 of commercially available authenticated standards.

562 The phenolic compound profiles in root extracts included coumarins and
563 coumarinolignans, and were markedly dependent of the plant growth pH (Figure 5); no
564 phenolics of the flavonoid and stilbene families were found. Under sufficient Fe supply, root
565 extracts from plants grown at pH 5.5 had mainly scopoletin hexoside (scopolin) and its
566 aglycon (scopoletin) as well as the coumarin precursor hexoside of ferulic acid. When Fe-
567 sufficient plants were grown at pH 7.5, no significant changes were found for ferulic acid
568 hexoside, scopolin, scopoletin and fraxetin and isofraxidin hexosides, whereas other
569 coumarins increased (including fraxetin, isofraxidin and the coumarinolignans cleomiscosins
570 A, B, C and D).

571 Iron deficiency changed markedly the coumarin/coumarinolignan profiles in root extracts
572 (Figure 5). In plants grown at pH 5.5 the profiles were similar under Fe deficiency or
573 sufficiency conditions, with moderate increases in fraxetin, isofraxidin hexosides and their
574 aglycones (fraxetin, isofraxidin and fraxinol), as well as of the cleomiscosins A, B, C and D.
575 However, in plants grown at pH 7.5 Fe deficiency caused a marked increase of all coumarin
576 hexosides, their aglycones and all coumarinolignans. When compared to their concentration
577 in Fe-sufficient plants at pH 7.5, the largest increase was 18-fold for cleomiscosin D,
578 followed by 13-fold for isofraxidin, 12-fold for fraxinol and the cleomiscosins A, B and C, 9-
579 fold for the hexoside of isofraxidin, 7-fold for the hexoside of fraxetin and the aglycone
580 fraxetin, 5-fold for scopoletin, and 2-fold for both scopolin and ferulic acid hexoside.

581 The most abundant coumarin in root extracts, irrespective of the growth conditions, was
582 scopoletin (Figure 6a). Summing up the two forms detected, the hexoside and aglycone,
583 scopoletin was 90-100% of the total coumarins, depending on the root conditions, with the
584 aglycone form being always predominant (85-93%) (Supplementary Figure S4b). In the case
585 of fraxetin, the aglycone was also the predominant form (at least 73-76%) in root extracts
586 from plants grown at pH 7.5, whereas in plants grown in absence of Fe at pH 5.5, only 24% of
587 the total fraxetin occurred in the aglycone form. In the case of isofraxidin the hexoside form
588 was predominant, with the aglycone accounting for 23-46% of the total depending on the
589 growth conditions (Supplementary Figure S4b).

590 **3.6 Coumarin and Coumarinolignan Concentrations in the Nutrient Solution**

591 The concentrations of coumarins and coumarinolignans were determined in the nutrient
592 solution of Fe-deficient plants after 7 and 14 days after imposing Fe deficiency (nutrient
593 solutions were renewed on day 7) (Figure 7). No determinations could be made in nutrient
594 solutions of Fe-sufficient plants due to the presence of Fe(III)-EDDHA, which causes the
595 overloading of C₁₈ materials. Coumarin hexosides were only occasionally detected at trace
596 levels (data not shown). When plants were grown at pH 5.5, the growth media at d 7
597 contained low concentrations of aglycones (scopoletin, fraxetin, isofraxidin and fraxinol;
598 Figure 7) and coumarinolignans (cleomiscosins A, C and D as well as the putative 5'-
599 hydroxycleomiscosin; Figure 7). After 14 d of Fe deficiency no significant changes were
600 observed. In contrast, when plants were grown at pH 7.5, the concentration of coumarins and
601 coumarinolignans in the nutrient solution were much higher than that found in the culture
602 medium of plant grown at pH 5.5 (Figure 7). When compared to the concentrations found
603 with Fe-deficient plants at pH 5.5, increases were large for scopoletin (6- and 12-fold at day 7
604 and 14, respectively) and very large for the rest of phenolics (in the range from 17- to 537-

605 fold). In addition, when Fe-deficient plants were grown at pH 7.5, the concentrations of
606 coumarins (with the exception of isofraxidin) and coumarinolignans in the nutrient solution
607 increased with time. When compared to the concentrations at d 7, increases at d 14 were 12-
608 fold for isofraxidin, 9-fold for fraxetin, 5-fold for cleomiscosin A, 3-fold for 5'-
609 hydroxycleomiscosins and the cleomiscosins B and D, and 2-fold for scopoletin and
610 cleomiscosin C.

611 Scopoletin was the predominant coumarin only at pH 5.5 after 7 d of Fe deficiency (86%
612 of the total coumarins), whereas at 14 d scopoletin and fraxetin accounted for 58 and 41% of
613 the total, respectively (Figure 6a). At pH 7.5 scopoletin and fraxetin were the major
614 coumarins at d 7 (57 and 31%, respectively), whereas at d 14 scopoletin, fraxetin and
615 isofraxidin accounted for 26, 53 and 20% of the total, respectively.

616 3.7 Allocation of Coumarins to the Roots and the Nutrient Solutions

617 The allocation of coumarins produced by Fe-deficient plants was affected by the growth
618 media pH. In plants grown at pH 5.5, only 19% of the total amount of coumarins was
619 allocated to the nutrient solution, whereas for plants grown at pH 7.5 coumarins were
620 allocated equally between nutrient solutions (51% of the total per plant) and roots (49%)
621 (Figure 6b). Fraxetin was preferentially allocated to the nutrient solution at both pH values,
622 whereas isofraxidin and fraxinol did only so at pH 7.5.

623 3.8 Mobilization of Fe from Fe(III)-oxide promoted by coumarins

624 In order to understand the role that coumarins could play in Fe plant nutrition, their ability to
625 mobilize Fe from Fe(III)-oxide was measured in *in vitro* incubation assays. The experiments
626 were carried out with a poorly crystalline Fe(III)-oxide and 1.5 ml of an assay medium
627 containing 0 (blank) or 100 μM of coumarin and buffered at pH 5.5 or 7.5. Three out of the
628 four coumarins assayed (scopoletin, isofraxidin and fraxin) have a catechol moiety capped *via*
629 hydroxyl group methylation or hydroxyl group glucosylation, whereas the fourth coumarin,
630 fraxetin, bears an available catechol moiety (see structures in Figure 1). Coumarolignans
631 could not be used in these experiments because of the lack of commercial authenticated
632 standards. Assays were run in the presence of the Fe(II) trapping agent BPDS to monitor the
633 reductive dissolution of Fe(III)-oxide, and the concentration of Fe(II)-BPDS₃ was termed
634 Fe(II). The overall mobilization of Fe was assessed by determining the total Fe in solution
635 using ICP-MS (Figure 8). The Fe mobilized by the buffer solutions (blanks) was on the
636 average 0.2 nmol Fe g⁻¹ Fe(III)-oxide min⁻¹. When the assay medium contained the non-
637 catechol coumarins fraxin, scopoletin and isofraxidin, the total Fe mobilized was in the range
638 0.9-1.2 nmol Fe g⁻¹ Fe(III)-oxide min⁻¹ (depending on the coumarins and the assay pH) and no
639 statistically significant differences were found when compared to the blank (Figure 8a).
640 However, when the assay medium contained the catechol coumarin fraxetin, the amounts of
641 Fe mobilized (5.8 and 9.4 nmol Fe g⁻¹ Fe(III)-oxide min⁻¹ for the assays at pH 5.5 and pH 7.5,
642 respectively) were significantly higher than the blank values (Figure 8a). Furthermore, the
643 total mobilization of Fe promoted by fraxetin at pH 7.5 increased linearly when the
644 concentration of fraxetin increased from 10 to 100 μM . A relevant fraction (40-44%) of the
645 mobilized Fe was trapped by BPDS and this fraction also increased linearly when the
646 concentration of fraxetin increased from 10 to 100 μM (Figure 8b).

647 4 Discussion

648 *Arabidopsis thaliana* plants produce and secrete an array of phenolics in response to Fe

649 deficiency when the pH of the nutrient solution is high. Phenolics found in this study include
650 several coumarinolignans not previously reported in *A. thaliana* (cleomiscosins A, B, C and D
651 and the 5'-hydroxycleomiscosins A and/or B), as well as other previously reported coumarins
652 (scopoletin, fraxetin, isofraxidin and fraxinol) and some coumarin precursors (ferulic acid and
653 coniferyl and sinapyl aldehydes). The identification of all these phenolic compounds was
654 achieved through an integrative interpretation of analytical data, including exact molecular
655 mass-to-charge ratios (m/z), low and high-resolution MSⁿ spectra, chromatographic RTs and
656 fluorescence/UV-VIS data. Furthermore, we report here for the first time on the quantification
657 of all identified coumarins, revealing that Fe deficiency mainly induced the root accumulation
658 and exudation of the non-catechol coumarin scopoletin and the catechol coumarin fraxetin,
659 with the exudation of fraxetin being more prominent when Fe chlorosis was intense. Also, we
660 show for the first time that fraxetin, but not scopoletin, was effective to mobilize Fe from an
661 scarcely soluble Fe(III)-oxide.

662 This is the first time cleomiscosins and 5'-hydroxycleomiscosins have been reported in *A.*
663 *thaliana*. Cleomiscosins were found in both roots and nutrient solutions, whereas 5'-
664 hydroxycleomiscosins were found only in nutrient solutions (Figures 5b, 7b). All
665 coumarinolignans found have a fraxetin moiety linked to different phenylpropanoid units
666 (Figure 1c). Non-conventional lignans, including coumarinolignans and other hybrid ones,
667 harbor a single phenylpropanoid unit, whereas conventional ones consist in phenylpropanoid
668 dimers. The common coumarin moiety in the coumarinolignans found, fraxetin, has been
669 consistently reported to increase with Fe deficiency in roots and growth media of *A. thaliana*
670 (Figures 5, 7; Fourcroy et al., 2014; Schmid et al., 2014; Schmidt et al., 2014). The
671 phenylpropanoid units found are the primary lignin precursors coniferyl (in cleomiscosins A
672 and B) and sinapyl alcohols (in cleomiscosins C and D), and the non-canonical monolignol 5-
673 hydroxyconiferyl alcohol (in 5'-hydroxycleomiscosins A and B) (Begum et al., 2010) (Figure
674 1c). Previously, two other coumarinolignans, composed of esculetin and either coniferyl
675 alcohol or sinapyl alcohol, were tentatively identified in *A. thaliana* root exudates (Strehmel
676 et al., 2014). Until now, cleomiscosins have been only reported in seeds and stem wood and
677 bark of various plant species, whereas 5'-hydroxycleomiscosins A and B were found in
678 *Mallotus apelta* roots (Xu et al., 2008) and *Eurycorymbus cavaleriei* twigs (Ma et al., 2009),
679 respectively. Cleomiscosin A has been reported in 22 plant species belonging to 12 families
680 (e.g., Sapindaceae and Simaroubaceae), whereas cleomiscosins B, C and D, although less
681 common, have been found in 6-10 plant species belonging to 5-9 families (Begum et al.,
682 2010).

683 Besides coumarinolignans, ferulic acid and other related metabolites were found to
684 accumulate in roots of Fe-deficient *A. thaliana* plants when grown at high pH (Table 1 and
685 Figure 5a). This is consistent with Fe-deficient *A. thaliana* root transcriptomic (Rodríguez-
686 Celma et al., 2013), proteomic (Lan et al., 2011) and metabolite data (Fourcroy et al., 2014):
687 (i) ferulic acid can be converted to feruloyl-CoA by the action of 4-coumarate:CoA ligases
688 (4CL1 and 4CL2), two enzymes that have been found to be robustly induced by Fe deficiency
689 (Lan et al., 2011; Rodríguez-Celma et al., 2013), (ii) feruloyl-CoA is a key precursor in the
690 biosynthesis of scopoletin (Kai et al., 2008), which accumulates in roots of Fe-deficient plants
691 (Figures 5a, 7a; Fourcroy et al., 2014; Schmid et al., 2014; Schmidt et al., 2014), and (ii)
692 ferulic acid hexoside has been reported to occur in Fe-deficient roots (Fourcroy et al., 2014).
693 Also, two other metabolites, coniferyl and sinapyl aldehydes, were occasionally found in Fe-
694 deficient roots (in the aglycone and hexoside forms, Tables 1, 3). Coniferyl aldehyde can
695 either lead to scopoletin biosynthesis *via* oxidation to ferulic acid (Kai et al., 2008) or be
696 reduced to coniferyl alcohol (Fraser and Chapple 2011), a precursor of lignin and lignans

697 (Barros et al., 2015), including cleomiscosins A and B. Sinapyl aldehyde is an intermediate
698 metabolite in the synthesis of lignin and lignans such as cleomiscosins C and D (Barros et al.,
699 2015), and may (assuming that isofraxidin synthesis is analogous to that of scopoletin, as
700 proposed by Petersen et al., 1999) be a precursor of the coumarin isofraxidin, which
701 accumulates consistently in Fe-deficient roots (Figure 5a).

702 Coumarins also accumulate in *A. thaliana* roots along with coumarinolignans and are
703 secreted to the growth media in response to Fe deficiency, especially when pH was high. Four
704 coumarins (scopoletin, fraxetin, isofraxidin and the isofraxidin isomer fraxinol) were found in
705 both root extracts and nutrient solutions (Tables 1, 2) confirming previous results (Fourcroy et
706 al., 2014; Schmid et al., 2014; Schmidt et al., 2014) (Supplementary Table S1). We could
707 identify fraxinol (annotated in a previous study as methoxyscopoletin; Fourcroy et al., 2014),
708 using an authenticated standard. Aglycones and hexose conjugates of the four coumarins were
709 found in roots (Figure 5 and Supplementary Figure S4b), whereas only the aglycone forms
710 were quantifiable in nutrient solutions, with hexoside forms being detected only occasionally
711 and in low amounts (Figure 7). We did not detect three more coumarins, esculetin, isofraxetin
712 and dihydroxyscopoletin, previously found as aglycones and/or glycoside forms by Schmid et
713 al. (2014) and/or Schmidt et al. (2014) in roots or exudates of Fe-deficient *A. thaliana*. This
714 could be due to differences in protocols for exudate collection and isolation of organic
715 compounds from the growth/exudation media or plant growth conditions. In any case, from
716 the published data it seems that the relative amount of these three coumarins was very low: in
717 the only study where quantification of some coumarins was carried out, the amount of
718 esculetin was 0.1% (roots) and <1% (exudates) when compared to those of scopoletin
719 (Schmid et al., 2014). Assuming similar ratios in our study, the concentration of esculetin
720 would be approximately 0.2-0.5 nmol g⁻¹ root FW in roots and nutrient solutions,
721 respectively, values still lower than those of fraxinol, the less abundant of the coumarins
722 detected in this study (Figures 5, 7). Regarding the other two coumarins not detected in this
723 study, isofraxetin and dihydroxyscopoletin, they were only detected in Schmid et al. (2014)
724 and Schmidt et al. (2014), respectively, indicating that their occurrence in Fe-deficient plants
725 is not consistent.

726 High pH induces by itself a certain Fe stress that results in the synthesis of phenolics in
727 roots. The increase in the production of some phenolic compounds was already observed in
728 Fe-sufficient plants grown at high pH (Figure 5 and Supplementary Figure S4a), along with
729 decreases in root and shoot Fe contents (Figure 2c) and increases in *FRO2* expression (Figure
730 2d), even when leaf Chl and biomass were not affected (Figure 2a,b,c). It was already known
731 that high pH compromises the root Fe acquisition from Fe(III)-chelates, with FCR activities
732 being much lower at pH 7.5 than at the optimal pH range of 5.0-5.5 (in *A. thaliana* and other
733 species; Moog et al., 1995; Susín et al., 1996), and FCR rates are known to be especially low
734 with highly stable chelates such as Fe(III)-EDDHA (Lucena, 2006). When plants were grown
735 in absence of Fe at pH 7.5 the Fe stress was much more intense and the synthesis of phenolics
736 in roots was fully enhanced (when compared with Fe-sufficient plants grown either at high or
737 low pH): concentrations of all phenolics in roots were much higher (Figure 5 and
738 Supplementary Figure S4a), the concentration of phenolics in the nutrient solution increased
739 markedly with time (Figure 7 and Supplementary Figure S4a), and there were marked
740 decreases in leaf Chl (Figure 2a,b), shoot biomass and shoot and root Fe contents (Figure 2c).
741 The high pH/zero Fe effect is rapid, since only after 3 d roots already showed an increased
742 expression of genes coding for root coumarin synthesis (*COMT*, *CCoAMT* and *F6'H1*) and Fe
743 acquisition components (*IRT1* and *FRO2*) (when compared with Fe-sufficient plants grown
744 either at high or low pH) (Figure 2d). In contrast, when plants were grown in absence of Fe at

745 pH 5.5, there was no effect on biomass (Figure 2c) and the decreases in leaf Chl and shoot
746 and root Fe contents (when compared with Fe-sufficient plants grown either at high or low
747 pH) were as large as those found at high pH (Figure 2a,b,c), and only moderate effects were
748 found with respect to phenolics, including: i) increases of some phenolics in roots (fraxetin,
749 isofraxidin, fraxinol, cleomiscosins A, C and D) (Figure 5 and Supplementary Figure S4a); ii)
750 time dependent increases in the concentration of all phenolics in the nutrient solution,
751 although concentrations were always lower than those found at high pH (Figure 7 and
752 Supplementary Figure S4a), and iii) a rapid (at 3 d) root increased expression of genes for Fe
753 root uptake, although to a much lower extent than at high pH, without any change in the
754 expression of genes involved in coumarin synthesis (Figure 2d).

755 Iron-supply and nutrient solution pH affect the relative coumarin concentrations in root
756 extracts and growth media. Whereas the non-catechol coumarin scopoletin was initially the
757 most abundant coumarin in root extracts and growth media, the catechol coumarin fraxetin
758 was progressively more abundant with time in the growth media of plants grown with zero Fe
759 (Figure 6). When other authors used HPLC-fluorescence for quantification, scopoletin was
760 found to be the most abundant coumarin in the growth media of Fe-deficient *A. thaliana*
761 (Schmid et al. 2014); fraxetin was not quantified in that study, possibly due to the very low
762 fluorescence rate of this compound. The extremely low fluorescence of fraxetin in
763 comparison with those of other coumarins (scopoletin, isofraxidin and esculetin) in the
764 growth media of Fe-deficient *A. thaliana* plants is shown in Supplementary Figure S5.
765 Interestingly, in the roots of Fe-deficient plants grown at pH 7.5 the coumarins that have a
766 larger aglycone fraction (scopoletin and fraxetin; Supplementary Figure S4b), likely due to
767 the action of a glucosidase, were also the prevalent ones in the growth media, supporting that
768 the aglycone forms are likely to be the substrate for the plasma membrane transporter
769 ABCG37. In this respect, the β -glucosidase *bglu42* is induced by Fe deficiency in roots
770 (García et al., 2010; Yang et al., 2010; Lan et al., 2011; Rodríguez-Celma et al., 2013), and
771 the roots of Fe-deficient *bglu42 A. thaliana* mutant plants apparently fail to secrete coumarins
772 (Zamioudis et al., 2014). However, coumarin glucosides such as scopolin have been reported
773 to occur in the exudates of Fe-deficient *A. thaliana* in other studies (Schmid et al., 2014;
774 Schmidt et al., 2014).

775 The structural features of each coumarin-type compound may confer specific roles that
776 contribute to the adaptation of *A. thaliana* to low Fe availability in alkaline conditions. The
777 catechol moiety enable coumarins to mobilize efficiently Fe from an Fe(III)-oxide (Figure
778 8a). Fraxetin, a coumarin bearing a catechol moiety and a methoxy substituent, mobilized
779 much more Fe than any of the non-catechol coumarins tested at the same concentration (100
780 μ M; scopoletin, isofraxidin and fraxin) at physiologically relevant pH values (5.5 and 7.5).
781 Specific structural features of the non-catechol coumarins tested, such as the O-glucosyl
782 moiety (in fraxin) and one or two methoxy groups (in scopoletin/fraxin and ixofraxidin,
783 respectively) do not appear to affect to the Fe mobilization ability of the coumarin, since these
784 three coumarins mobilized similar amounts of Fe (Figure 8a). This confirms what has been
785 reported previously (at pH 7.2) with the catechol coumarin esculetin (no methoxy substituent)
786 and the non-catechol coumarins scopoletin (one methoxy and one hydroxy substituents) and
787 esculin (one O-glucosyl and one hydroxy substituents) (Schmid et al., 2014). In addition, the
788 present study revealed that the mobilization of Fe from Fe(III)-oxide promoted by fraxetin
789 involves a significant reduction of Fe(III) to Fe(II) and appears to be controlled by the
790 fraxetin concentration and the medium pH. Approximately 42% of the Fe mobilized by
791 fraxetin was trapped by BPDS, regardless of the assay pH and the fraxetin concentration
792 (Figure 8). The Fe(II) produced may be directly taken up by root cells, chelated by other

793 natural ligands and/or re-oxidized to Fe(III). The amount of Fe mobilized by fraxetin was 1.6-
794 fold higher at pH 7.5 -typical of calcareous soils- than at pH 5.5 (Figure 8a). Also, increases
795 in fraxetin concentration (from 10 to 100 μM) led to a marked enhancement in Fe
796 mobilization rates (Figure 8b). Most of the fraxetin produced by Fe-deficient plants (80-90%)
797 was allocated to the nutrient solution regardless of the growth media pH, in contrast with the
798 small amount of the non-catechol coumarin, scopoletin, allocated to the nutrient solution (12-
799 23%) (Figure 6b). Taking also into account the concentrations estimated for scopoletin (21
800 μM), fraxetin (43 μM), isofraxidin (14 μM) and fraxinol (0.5 μM) in the soil solution
801 surrounding the root (apex) of *A. thaliana* growing without Fe at pH 7.5 (calculated as in
802 Römheld, 1991, for phytosiderophores), it seems likely that fraxetin could play a role as an Fe
803 mobilizer in natural conditions. A catechol group is also present in the coumarinolignans 5'-
804 hydroxycleomiscosins A and B (Figure 1c) that were found only in exudates (Table 1 and
805 Figure 7). Therefore, not only fraxetin but also 5-hydroxycleomiscosins A/B may have a role
806 in mining Fe from soil Fe sources at high pH, providing soluble Fe for plant uptake.
807 Unfortunately, no authenticated standards exist in the market for these compounds. On the
808 other hand, coumarins, having or not catechol groups, play a well-established role in plant
809 defense, serving as allelochemicals against a broad array of organisms (e.g., bacteria, fungi,
810 nematodes, insects, etc), with their synthesis being activated in plants after infection
811 (Weinmann, 1997; Bourgaud et al., 2006). Therefore, the array of coumarin-type compounds
812 found in the growth media could play multiple roles, achieving different benefits for Fe-
813 deficient plants.

814 Accumulating experimental evidences suggest that the Fe deficiency-elicited production of
815 coumarin-type phenolics allows *A. thaliana* plants interacting with the rhizosphere
816 microbiome, including beneficial and pathogen organisms. On one hand, Fe-deficient *A.*
817 *thaliana* plants display reduced susceptibility to infection with the necrotrophic fungus
818 *Botrytis cinerea* and the bacterial plant pathogen *Dickeya dadantii*, with an Fe
819 supplementation restoring symptoms severity (Kieu et al., 2012). On the other hand, the
820 activation of immunity towards broadly diverse pathogens and even insects and herbivores in
821 *A. thaliana* elicited by the beneficial rhizobacteria *Pseudomonas fluorescens* WCS417 and
822 mediated by the root-specific transcription factor MYB72 (Van der Ent et al., 2008; Segarra et
823 al., 2009), also required for the induction of Fe deficiency responses (Palmer et al., 2013),
824 involves not only the production of F6'H1-dependent coumarins but also their secretion
825 (Zamioudis et al., 2014). In fact, two *Arabidopsis* mutants failing in the production and/or
826 secretion of coumarins, *myb72* and *bglu42*, did not show, when grown in the presence of
827 WCS417, enhanced resistance against two biotrophic pathogens (the Gram-negative
828 bacterium *Pseudomonas syringae* pv. tomato DC3000 and the pseudo-fungus
829 *Hyaloperonospora arabidopsidis*; Zamioudis et al., 2014). Also, BGLU42 overexpression led
830 to a significantly enhanced resistance against *B. cinerea*, *H. arabidopsidis* and *P. syringae* pv.
831 tomato DC3000 (Zamioudis et al., 2014). The enhanced disease resistance of *A. thaliana*
832 against different pathogens can be associated with the structure of the coumarin-type
833 compounds produced, since different substituents in the backbone of coumarins and lignans
834 can influence biological activity (Weinmann 1997; Apers et al., 2003; Borges et al., 2005;
835 Zhang et al., 2014; Pilkington and Barker 2015).

836 Certain structural features of coumarins and coumarinolignans produced by roots of Fe-
837 deficient *A. thaliana* plants may confer specific roles in shaping the rhizosphere microbiome.
838 In fact, the existence of differences in inhibitory potential against specific microorganisms
839 may be expected in Fe deficiency-induced coumarins. First, all coumarins detected in Fe-
840 deficient *A. thaliana* root extracts and exudates are highly oxygenated and with

841 hydroxyl/methoxy substituents: scopoletin and esculetin are di-oxygenated and fraxetin,
842 fraxetin isomer, isofraxidin and fraxinol are tri-oxygenated (Figure 1a). A high number of
843 oxygen-containing substituents in the benzopyrone coumarin backbone (Figure 1a) appears to
844 be determinant for broadening the antibacterial spectrum (Kayser and Kolodziej, 1999),
845 whereas the presence of simple substituents (*e.g.*, hydroxy, methoxy) instead of bulkier chains
846 may aid bacterial cell wall penetration. Second, an oxygenation pattern consisting in two
847 methoxy substituents and at least one additional hydroxyl substituent is present in the minor
848 tri-oxygenated coumarins isofraxidin and fraxinol produced by Fe-deficient *A. thaliana* roots.
849 This oxygenation pattern seems to confer to tri-oxygenated coumarins a strong and wide
850 inhibitory activity against Gram-positive and Gram-negative bacteria (Kayser and Kolodziej
851 1999; Smyth et al., 2009). Furthermore, the estimated concentrations of scopoletin, fraxetin,
852 isofraxidin and fraxinol in the soil solution surrounding the root (apex) of *A. thaliana* growing
853 without Fe at pH 7.5 (see above) are close or above the minimum inhibitory concentration of
854 di- and tri-oxygenated coumarins against Gram-positive and Gram-negative bacteria (1.3-11.2
855 and 0.9-4.5 μM , respectively; Kayser and Kolodziej 1999).

856 Regarding plant coumarinolignans, the current knowledge on their biological activities is
857 mostly pharmacological, derived from the ethno-medical utilization of some plant species
858 (Begum et al., 2010; Zhang et al., 2014; Pilkington and Barker 2015). Known activities of
859 cleomiscosins include liver protection, cytotoxicity against lymphocytic leukemia cells,
860 immunomodulation, and others. In plants, the defense roles for conventional lignans have
861 been studied, and certain structural features appear to affect the activities against specific
862 organisms. First, coumarinolignans are more aromatic than conventional lignans, suggesting
863 they may have a higher effectiveness. For instance, increased antifungal activities were
864 observed when the phenyl ring in a monomeric phenylpropanoid derivative was replaced by
865 naphthyl or phenanthryl rings, whereas no or very low antifungal activity is associated to the
866 monomeric phenylpropanoid moieties in conventional lignans (Apers et al., 2003). Second,
867 the occurrence of methoxy substituents in lignans appear confer stronger insecticide and
868 fungicide activities, whereas the presence of polar substituents, especially hydroxy or
869 glycoside groups, sometimes reduced them (Harmatha and Nawrot 2002; Harmatha and
870 Dinan 2003; Kawamura et al., 2004). Since cleomiscosin structures differ in the methoxy and
871 hydroxy substituents (Figure 1c), their possible insecticide and fungicide activities is likely to
872 be different.

873 Results presented here highlight that Fe deficiency elicits the accumulation in roots and
874 secretion into the growth media of an array of coumarin-type compounds, including
875 coumarinolignans (cleomiscosins A, B, C and D and the 5'-hydroxycleomiscosins A and/or
876 B) and simple coumarins (scopoletin, fraxetin, isofraxidin and fraxinol) in *A. thaliana*. The
877 phenolics response was much more intense when the plant accessibility to Fe was decreased
878 and Fe status deteriorated, as it occurs when plants are grown in the absence of Fe at pH 7.5.
879 The structural features of the array of coumarins and lignans produced and their
880 concentrations in roots and growth media suggest that they may play dual, complementary
881 roles as Fe(III) mobilizers and allelochemicals. Fraxetin, a catechol coumarin, was the most
882 prominent coumarin found in the growth media of Fe-deficient *A. thaliana* plants grown at
883 high pH and was especially effective in mobilization of Fe from an Fe(III)-oxide. In contrast,
884 the rest of coumarins were non-catechols and were present in much lower concentrations, and
885 therefore their role in mobilizing Fe is unlikely, although they can still be efficient as
886 allelochemicals. Therefore, the production and secretion of phenolics by roots in response to
887 Fe deficiency would promote an overall decrease in the competition for Fe in the immediate
888 vicinity of roots, resulting in an improved plant Fe nutrition. Results also suggest that Fe

889 deficiency could be a good experimental model to understand the ecological dynamics of the
890 biotic interactions in the plant rhizosphere.

891 **5 Conflict of Interest Statement**

892 The authors declare that the research was conducted in the absence of any commercial or
893 financial relationships that could be construed as a potential conflict of interest.

894 **6 Authors contributors**

895 AA-F, PF and AA conceived and designed the experiments, PS-T conducted experiments,
896 collected data, and drafted the manuscript, AL-V quantified phenolics, carried out Fe
897 mobilization studies and made figures, AA, FG, J-FB, JA and AA-F wrote, reviewed and
898 edited the paper. All authors read and approved the final manuscript.

899 **7 Funding**

900 Work supported by the Spanish Ministry of Economy and Competitiveness (MINECO) (grant
901 AGL2013-42175-R, co-financed with FEDER) and the Aragón Government (group A03). PS-
902 T and AL-V were supported by MINECO-FPI contracts.

903 **8 Acknowledgements**

904 We thank Cristina Ortega and Gema Marco (Aula Dei Experimental Station-CSIC) for
905 growing and harvesting plants.

906 **9 Supplementary Material**

907 Supplementary data for this article can be found online at:
908

909 **10 References**

- 910 Abadía, J., and Abadía, A. (1993). "Iron and plant pigments", in *Iron Chelation in Plants and*
911 *Soil Microorganisms*, eds. L.L Barton and B.C. Hemming (New York, NY: Academic
912 Press), 327-343.
- 913 Apers, S., Vlietinck, A., and Pieters, L. (2003). Lignans and neolignans as lead compounds.
914 *Phytochem. Rev.* 2, 201-217.
- 915 Aznar, A., Chen, N.W.G., Thomine, S., and Dellagi, A. (2015). Immunity to plant pathogens
916 and iron homeostasis. *Plant Sci.* 240, 90-97.
- 917 Barros, J., Serk, H., Granlund, I., and Pesquet, E. (2015). The cell biology of lignification in
918 higher plants. *Ann. Bot.* 115, 1053-1074.
- 919 Begum, S.A., Sahai, M., and Ray, A.B. (2010). Non-conventional lignans: coumarinolignans,
920 flavonolignans, and stilbenolignans. *Fort. Chem. Org. Nat.* 93, 1-70.
- 921 Borges, F., Roleira, F., Milhazes, N., Santana, L., and Uriarte, E. (2005). Simple coumarins
922 and analogues in medicinal chemistry: occurrence, synthesis and biological activity.
923 *Curr. Med. Chem.* 12, 887-916.
- 924 Briat, J.F., Dubos, C., and Gaymard, F. (2015). Iron nutrition, biomass production, and plant
925 product quality. *Trends Plant Sci.* 20, 33-40.
- 926 Bristow, A.W.T. (2006). Accurate mass measurement for the determination of elemental
927 formula A tutorial. *Mass Spectrom. Rev.* 25, 99-111.
- 928 Bourgaud, F., Hehn, A., Larbat, R., Doerper, S., Gontier, E., Kellner, S., and et al., (2006).

929 Biosynthesis of coumarins in plants: a major pathway still to be unravelled for
930 cytochrome P450 enzymes. *Phytochem. Rev.* 5, 293-308.

931 Cesco, S., Neumann, G., Tomasi, N., Pinton, R., and Weisskopf, L. (2010). Release of plant-
932 borne flavonoids into the rhizosphere and their role in plant nutrition. *Plant Soil* 329, 1-
933 25.

934 Chattopadhyay, S.K., Kumar, S., Tripathi, S., Kaur, R., Tandon, S., and Rane, S. (2008).
935 High-performance liquid chromatography and LC-ESI-MS method for the identification
936 and quantification of two biologically active isomeric coumarinolignoids cleomiscosin
937 A and cleomiscosin B in different extracts of *Cleome viscosa*. *Biomed. Chromatogr.* 22,
938 1325-1345.

939 Cheng, X.F., and Chen, Z.L. (2000). Coumarinolignoids of *Mallotus apelta*. *Fitoterapia* 71,
940 341-342.

941 Croteau, R., Kutchan, T.M., and Lewis, N.G. (2000). "Natural products (secondary
942 metabolites)", in *Biochemistry and Molecular Biology of Plants*, eds. B. Buchanan, W.
943 Gruissem, and R. Jones (Rockville, MD: American Society of Plant Physiologists),
944 1250-1318.

945 Crumbliss, A.L., and Harrington, J.M. (2009). Iron sequestration by small molecules:
946 thermodynamic and kinetic studies of natural siderophores and synthetic model
947 compounds. *Adv. Inorg. Chem.* 61, 179-250.

948 Fraser, C.M., and Chapple, C. (2011). The phenylpropanoid pathway in Arabidopsis.
949 *Arabidopsis Book* 9, e0152.

950 Fourcroy, P., Sisó-Terraza, P., Sudre, D., Savirón, M., Reyt, G., Gaymard, F., et al., (2014).
951 Involvement of the ABCG37 transporter in secretion of scopoletin and derivatives by
952 Arabidopsis roots in response to iron deficiency. *New Phytol.* 201, 155-167.

953 Fourcroy, P., Tissot, N., Reyt, G., Gaymard, F., Briat, J.F., and Dubos, C. (2016). Facilitated
954 Fe nutrition by phenolic compounds excreted by the Arabidopsis ABCG37/PDR9
955 transporter requires the IRT1/FRO2 high-affinity root Fe²⁺ transport system. *Mol. Plant*
956 9, 485-488.

957 García, M.J., Lucena, C., Romera, F.J., Alcántara, E., and Pérez-Vicente, R. (2010). Ethylene
958 and nitric oxide involvement in the up-regulation of key genes related to iron
959 acquisition and homeostasis in Arabidopsis. *J. Exp. Bot.* 61, 3885-3899.

960 Guerinot, M.L., and Ying, Y. (1994). Iron: Nutritious, noxious, and not readily available.
961 *Plant Physiol.* 104, 815-820.

962 Harmatha, J., and Nawrot, J. (2002). Insect feeding deterrent activity of lignans and related
963 phenylpropanoids with a methylenedioxyphenyl (piperonyl) structure moiety. *Entomol.*
964 *Exp. Appl.* 104, 51-60.

965 Harmatha, J., and Dinan, L. (2003). Biological activities of lignans and stilbenoids associated
966 with plant-insect chemical interaction. *Phytochem. Rev.* 2, 321-330.

967 Jin, C.W., He, Y.F., Tang, C.X., Wu, P., and Zheng, S.J. (2006). Mechanisms of microbially
968 enhanced Fe acquisition in red clover (*Trifolium pratense* L.). *Plant Cell Environ.* 29,
969 888-897.

970 Jin, C.W., Ye, Y.Q., and Zheng S.J. (2014). An underground tale: contribution of microbial
971 activity to plant iron acquisition via ecological processes. *Ann. Bot.* 113, 7-18.

972 Jin, C.W., You, G.Y., He, Y.F., Tang, C.X., Wu, P. and Zheng, S.J. (2007) Iron deficiency-
973 induced secretion of phenolics facilitates the reutilization of root apoplastic iron in red
974 clover. *Plant Physiol.* 144: 278-285.

975 Kai, K., Mizutani, M., Kawamura, N., Yamamoto, R., Tamai, M., Yamaguchi, H., et al.,
976 (2008). Scopoletin is biosynthesized *via* ortho-hydroxylation of feruloyl CoA by a 2-
977 oxoglutarate-dependent dioxygenase in *Arabidopsis thaliana*. *Plant J.* 55, 989-999.

- 978 Kayser, O., and Kolodziej, H. (1999). Antibacterial activity of simple coumarins: structural
979 requirements for biological activity. *Z. Naturforsch. C* 54, 169-174.
- 980 Kaur, R., Kumar, S., Chatterjee, A., and Chattopadhyay, S.K. (2010). High-performance
981 liquid chromatographic method for identification and quantification of three potent liver
982 protective coumarinolignoids-cleomiscosin A, cleomiscosin B and cleomiscosin C-in
983 extracts of *Cleome viscosa*. *Biomed. Chromatogr.* 24, 1000-1005.
- 984 Kawamura, F., Ohara, S., and Nishida, A. (2004). Antifungal activity of constituents from the
985 heartwood of *Gmelina arborea*: Part 1. Sensitive antifungal assay against
986 Basidiomycetes. *Holzforschung* 58, 189-192.
- 987 Kieu, N.P., Aznar, A., Segond, D., Rigault, M., Simond-Côte, E., Kunz, C., Soulie, M.C.,
988 Expert, D., and Dellagi, A. (2012). Iron deficiency affects plant defense responses and
989 confers resistance to *Dickeya dadantii* and *Botrytis cinerea*. *Mol. Plant Pathol.* 13, 816-
990 827.
- 991 Kobayashi, T., and Nishizawa, N.K. (2012). Iron uptake, translocation, and regulation in
992 higher plants. *Annu. Rev. Plant Biol.* 63, 131-52.
- 993 Lan, P., Li, W.F., Wen, T.N., Shiau, J.Y., Wu, Y.C., Lin, W.D., and Schmidt, W. (2011).
994 iTRAQ Protein profile analysis of Arabidopsis roots reveals new aspects critical for iron
995 homeostasis. *Plant Physiol.* 155, 821-834.
- 996 Larbi, A., Abadía, A., Morales, F., and Abadía, J. (2004). Fe resupply to Fe-deficient sugar
997 beet plants leads to rapid changes in the violaxanthin cycle and other photosynthetic
998 characteristics without significant de novo chlorophyll synthesis. *Photosynth. Res.* 79,
999 59-69.
- 1000 Le Roy, J., Huss, B., Creach, A., Hawkins, S., and Neutelings, G. (2016). Glycosylation is a
1001 major regulator of phenylpropanoid availability and biological activity in plants. *Front.*
1002 *Plant Sci.* 7, 735.
- 1003 Lindsay, W.L. (1995). "Chemical reactions in soils that affect iron availability to plants. A
1004 quantitative approach", in *Iron Nutrition in Soils and Plants*, ed. J. Abadía, (Dordrecht,
1005 The Netherlands: Kluwer Academic Publishers), 7-14.
- 1006 Lucena, J.J. (2006). "Synthetic iron chelates to correct iron deficiency in plants", in *Iron*
1007 *Nutrition in Plants and Rhizospheric Microorganisms*, eds. L.L. Barton, and J. Abadía
1008 (Dordrecht, The Netherlands: Springer), 103-128.
- 1009 Ma, Z., Zhang, X., Cheng, L., and Zhang, P. (2009). Three lignans and one coumarinolignoid
1010 with quinone reductase activity from *Eurycorymbus cavaleriei*. *Fitoterapia* 80, 320-
1011 326.
- 1012 Mimmo, T., Del Buono, D., Terzano, R., Tomasi, N., Vigani, G., Crecchio, C., et al., (2014).
1013 Rhizospheric organic compounds in the soil-microorganism-plant system: their role in
1014 iron availability. *Eur. J. Soil Sci.* 65, 629-642.
- 1015 Moog, P.R., van der Kooij, T.A.W., Brüggemann, W., Schiefelbein, J.W., and Kuiper, P.J.C.
1016 (1995). Responses to iron deficiency in *Arabidopsis thaliana*: The Turbo iron reductase
1017 does not depend on the formation of root hairs and transfer cells. *Planta* 195, 505-513.
- 1018 Palmer, C.M., Hindt, M.N., Schmidt, H., Clemens, S., and Guerinot, M.L. (2013). MYB10
1019 and MYB72 are required for growth under iron-limiting conditions. *Plos Genet.* 9,
1020 e1003953.
- 1021 Petersen, M., Strack, D., and Matern, U. (1999). "Biosynthesis of phenylpropanoid and
1022 related compounds", in *Biochemistry of Plant Secondary Metabolism*, ed. M. Wink
1023 (Sheffield, United Kingdom: Sheffield Academic Press Ltd), 151-221.
- 1024 Pilkington, L.I., and Barker, D. (2015). Synthesis and biology of 1,4-benzodioxane lignan
1025 natural products. *Nat. Prod. Rep.* 32, 1369-1388.
- 1026 Rodríguez-Celma, J., Lin, W.D., Fu, G.M., Abadía, J., López-Millán, A.F., and Schmidt, W.
1027 (2013). Mutually exclusive alterations in secondary metabolism are critical for the

1028 uptake of insoluble iron compounds by *Arabidopsis* and *Medicago truncatula*. *Plant*
1029 *Physiol.* 162, 1473-1485.

1030 Römheld, V. (1991). The role of phytosiderophores in acquisition of iron and other
1031 micronutrients in graminaceous species: An ecological approach. *Plant Soil* 130, 127-
1032 134.

1033 Schmid, N.B., Giehl, R.F.H., Doll, S., Mock, H.P., Strehmel, N., Scheel, D., et al., (2014).
1034 Feruloyl-CoA 6'-hydroxylase1-dependent coumarins mediate iron acquisition from
1035 alkaline substrates in *Arabidopsis*. *Plant Physiol.* 164, 160-172.

1036 Schmidt, H., Gunther, C., Weber, M., Sporlein, C., Loscher, S., Bottcher, C., et al., (2014).
1037 Metabolome analysis of *Arabidopsis thaliana* roots identifies a key metabolic pathway
1038 for iron acquisition. *Plos One* 9, 11.

1039 Segarra, G., Van der Ent, S., Trillas, I., and Pieterse, C.M.J. (2009). MYB72, a node of
1040 convergence in induced systemic resistance triggered by a fungal and a bacterial
1041 beneficial microbe. *Plant Biol.* 11, 90-96.

1042 Sisó-Terraza, P., Ríos, J.J., Abadía, J., Abadía, A., and Álvarez-Fernández, A. (2016). Flavins
1043 secreted by roots of iron-deficient *Beta vulgaris* enable mining of ferric oxide via
1044 reductive mechanisms. *New Phytol.* 209, 733-745.

1045 Smyth, T., Ramachandran, V.N., and Smyth, W.F. (2009). A study of the antimicrobial
1046 activity of selected naturally occurring and synthetic coumarins. *Int. J. Antimicrob. Ag.*
1047 33, 421-426.

1048 Strehmel, N., Böttcher, C., Schmidt, S., and Scheel, D. (2014). Profiling of secondary
1049 metabolites in root exudates of *Arabidopsis thaliana*. *Phytochemistry* 108, 35-46.

1050 Sun, H., Wang, L., Zhang, B., Ma, J., Hettenhausen, C., Cao, G., et al., (2014). Scopoletin is a
1051 phytoalexin against *Alternaria alternata* in wild tobacco dependent on jasmonate
1052 signaling. *J. Exp. Bot.* 65, 4305-4315.

1053 Susín, S., Abadía, A., González-Reyes, J.A., Lucena, J.J., and Abadía, J. (1996). The pH
1054 requirement for in vivo activity of the iron-deficiency-induced "Turbo" Ferric Chelate
1055 Reductase: A comparison of the iron-deficiency-induced iron reductase activities of
1056 intact plants and isolated plasma membrane fractions in sugar beet (*Beta vulgaris*).
1057 *Plant Physiol.* 110, 111-123.

1058 Van der Ent, S., Verhagen, B.W.M., Van Doorn, R., Bakker, D., Verlaan, M.G., Pel, M.J.C.,
1059 et al., (2008). MYB72 is required in early signaling steps of rhizobacteria-induced
1060 systemic resistance in *Arabidopsis*. *Plant Physiol.* 146, 1293-1304.

1061 Weinmann, I. (1997). *Coumarins: biology, applications and mode of action*. Chichester,
1062 United Kingdom: Wiley Press.

1063 Yang, T.J.W., Lin, W.D., and Schmidt, W. (2010). Transcriptional profiling of the
1064 *Arabidopsis* iron deficiency response reveals conserved transition metal homeostasis
1065 networks. *Plant Physiol.* 152, 2130-2141.

1066 Xu, J.F., Feng, Z.M., Liu, J., and Zhang, P.C. (2008). New hepatoprotective
1067 coumarinolignoids from *Mallotus apelta*. *Chem. Biodivers.* 5, 591-597.

1068 Zamioudis, C., Hanson, J., and Pieterse, C.M.J. (2014). β -Glucosidase BGLU42 is a MYB72-
1069 dependent key regulator of rhizobacteria-induced systemic resistance and modulates
1070 iron deficiency responses in *Arabidopsis* roots. *New Phytol.* 204, 368-379.

1071 Zhang, J., Chen, J.J., Liang, Z.Z., and Zhao, C.Q. (2014). New Lignans and their biological
1072 activities. *Chem. Biodivers.* 11, 1-54.

1073

1074 **Figure legends**

1075 **Figure 1** Chemical structures of some of the phenolic compounds cited in this study. The
1076 plant compounds include coumarins and their glucosides (a), coumarin precursors and
1077 monolignols (b) and coumarinolignans derived from the coumarin fraxetin (c). The fraxetin
1078 moiety is highlighted in blue in the coumarinolignan structures. Compounds used as internal
1079 standards (d) include a methylenedioxy-coumarin and a lignan.

1080 **Figure 2** Effects of Fe deficiency and high pH on plant Fe status, root Fe uptake machinery
1081 and phenylpropanoid pathway components in *Arabidopsis thaliana*. Plants were pre-grown
1082 for 11 d in the presence of 20 μM Fe (III)-EDTA at pH 5.5, and then grown for 14 d in a
1083 medium with 0 (-Fe) or 20 μM (+Fe) Fe(III)-EDDHA in nutrient solutions buffered at pH 5.5
1084 (with 5 mM MES-NaOH) or 7.5 (with 5mM HEPES-NaOH). (a) Plants at day 14 after
1085 imposing treatments. (b) Leaf chlorophyll concentration in young leaves of plants at day 14
1086 after imposing treatments; data are means \pm SE (n=3) and significant differences among
1087 treatments (at $p < 0.05$) are marked with different letters above the columns. (c) Dry weights
1088 and Fe contents in shoots and roots at day 14 after imposing treatments. Data are means \pm SE
1089 for biomass (n=5) and for Fe contents (n=2-5), and significant differences among treatments
1090 (at $p < 0.05$) are marked with different letters above the columns. (d) Abundance of *IRT1*,
1091 *FRO2*, *ABCG37* (*PDR9*), *F6'H1*, *COMT* and *CCoAMT* transcripts in roots at day 3 after
1092 imposing treatments. RNAs were extracted from roots and analyzed by qRT-PCR, using PP2
1093 (*At1g13320*) as housekeeping gene. The $\Delta\Delta\text{CT}$ method was used to determine the relative
1094 transcript level. Data are means \pm SE (n=3-5). For each gene, significant differences among
1095 treatments (at $p < 0.05$) are marked with different letters above the columns.

1096 **Figure 3** Chromatographic separation of a range of phenolic-type compounds produced in
1097 response to Fe deficiency by *Arabidopsis thaliana* roots. Typical fluorescence (at λ_{exc} 365 and
1098 λ_{em} 460 nm) and absorbance (at 320 nm) chromatograms for root and growth media extracts
1099 from plants grown as described in Fourcroy et al. (2014): plants were pre-grown for 29 d in
1100 the presence of 45 μM Fe (III)-EDTA at pH 5.5, and then grown for 7 d in a medium with 0 (-
1101 Fe) or 45 μM Fe (III)-EDTA (+Fe) (the pH was not readjusted to 5.5, with the final pH being
1102 *c.* 7.0 in all pots). Chromatograms were obtained using Elution program 1. The encircled
1103 numbers above each peak correspond to the phenolic compounds listed in Table 1. RU,
1104 relative units, AU absorbance units, and RT, retention time.

1105 **Figure 4** Identification of compounds 14-18, produced by Fe-deficient *Arabidopsis thaliana*
1106 roots, as coumarinolignans derived from fraxetin. (a) MS^2 spectra of compounds 14-18 and
1107 the cleomiscosins A (Cm A), B (Cm B), C (Cm C) and D (Cm D) isolated from *Cleome*
1108 *viscosa* seeds. (b) MS^2 spectra of fraxetin and MS^3 spectra of m/z 209 ion from the
1109 corresponding $[\text{M}+\text{H}]^+$ ions of compounds 14-18, Cm A, Cm B, Cm C and Cm D. Spectra
1110 were obtained from the HPLC/ESI-MS(ion trap) analyses of growth media extracts from Fe-
1111 deficient plants and a cleomiscosin isolate. (c) Typical HPLC-ESI-MS(TOF) chromatograms
1112 for growth media extracts from Fe-deficient plants and for the cleomiscosin isolate, extracted
1113 at m/z 403.10, 417.12 and 387.11 and with a precision of ± 0.02 m/z units. The encircled
1114 numbers in the spectra and above each chromatographic peak correspond to the phenolic
1115 compounds listed in Table 1.

1116 **Figure 5** Effects of Fe deficiency and high pH on the concentrations (in nmol g^{-1} root FW) of
1117 coumarins (a) and coumarinolignans (b) in *Arabidopsis thaliana* roots. Plants were pre-grown
1118 as indicated in Figure 2 and grown for 14 d with 0 (-Fe) or 20 μM Fe (+Fe) in nutrient

1119 solution buffered at pH 5.5 (with 5 mM MES-NaOH) or 7.5 (with 5 mM HEPES-NaOH). The
1120 concentrations of ferulic acid hexoside are expressed as fraxin. The levels of the
1121 cleomiscosins are expressed in peak area ratio, relative to the lignan matairesinol used as
1122 internal standard. Data are means \pm SE (n=3-5). For each compound, significant differences
1123 among treatments (at $p < 0.05$) are marked with different letters above the columns.

1124 **Figure 6** Effects of Fe deficiency, high pH and/or time on the relative concentrations of
1125 coumarins (scopletin, fraxetin, isofraxidin, fraxinol and total coumarins) in root extracts and
1126 nutrient solution (a) and on the allocation of coumarins to the roots and the nutrient solutions
1127 of *Arabidopsis thaliana* (b). Plants were pre-grown as indicated in Figure 2 and grown for 7
1128 or 14 d with 0 (-Fe) or 20 μ M Fe (+Fe) in nutrient solution buffered at pH 5.5 (with 5 mM
1129 MES-NaOH) or 7.5 (with 5 mM HEPES-NaOH). Data are means of n=3-5. The absolute
1130 values are shown in Figures 5 and 7.

1131 **Figure 7** Effects of time of Fe deficiency and high pH treatments on the concentrations (in
1132 nmol g^{-1} root FW) of coumarins (a) and coumarinolignans (b) in the nutrient solution of iron
1133 (Fe)-deficient *Arabidopsis thaliana*. Plants were pre-grown as indicated in Figure 2 and
1134 grown for 7 or 14 d with 0 μ M Fe in nutrient solution buffered at pH 5.5 (with 5 mM MES-
1135 NaOH) or 7.5 (with 5 mM HEPES-NaOH). The levels of the cleomiscosins are expressed in
1136 peak area ratio, relative to the lignan matairesinol used as internal standard. Data are means \pm
1137 SE (n=3-5). For each compound, significant differences among treatments (at $p < 0.05$) are
1138 marked with different letters above the columns. *5'-Hydroxyclemomiscosins A and/or B
1139 should be considered since separation of these isomer compounds might have not been
1140 achieved.

1141 **Figure 8** Iron mobilization from an scarcely soluble Fe(III)-oxide as affected by coumarins.
1142 (a) Structure-activity relationship of coumarins on Fe mobilization activity. The assays
1143 consisted in the incubation of 10 mg of Fe(III)-oxide with a solution of 0 (blank) or 100 μ M
1144 of the indicated coumarins and 600 μ M BPDS at two different pH values, 5.5 and 7.5. Total
1145 Fe and Fe(II)-(BPDS)₃ in solution were determined by ICP-MS and spectrophotometry,
1146 respectively. (b) Effects of the fraxetin concentration on the Fe mobilization activity at pH
1147 7.5. Scatter plot of the concentration of fraxetin *versus* the total Fe mobilized and the Fe(II),
1148 with linear regression lines in black and their corresponding equations. In all cases (a and b),
1149 data are means \pm SE (n = 3-12) and asterisks denote a statistically significant difference
1150 between blank and a coumarin-containing assay medium as determined by Student's t- test (P
1151 < 0.05).

In review

Table 1. Phenolic compounds secreted and accumulated by *Arabidopsis thaliana* roots in response to Fe deficiency: retention times (RT), exact mass-to-charge ratios (m/z), molecular formulae and error m/z (in ppm). The m/z ratios for $[M+H]^+$ and $[M-H]^-$ were determined from the HPLC-ESI-MS(TOF) data obtained in positive and negative mode, respectively. For compounds 3, 5, and 6 in positive mode, the m/z shown are those measured for the Na ($[M+Na]^+$) or K ($[M+K]^+$) adducts, because they were more intense than those for $[M+H]^+$. Common names for coumarins are also indicated in brackets.

Compound #	RT (min) program 1	RT (min) program 2	Measured m/z	Molecular formula	Calculated m/z	Error m/z (ppm)	Annotation
1	9.8	10.3	355.1028	$C_{16}H_{19}O_9^+$	355.1024	1.1	7-hydroxy-6-methoxycoumarin hexoside (scopolin, scopoletin hexoside)
			353.0877	$C_{16}H_{17}O_9^-$	353.0867	2.8	
2	10.0	10.6	357.1182	$C_{16}H_{21}O_9^+$	357.1180	0.6	ferulic acid hexoside
			355.1030	$C_{16}H_{19}O_9^-$	355.1024	1.7	
3	10.4	12.3	363.1055	$C_{16}H_{20}O_8Na^+$	363.1050	1.4	coniferyl aldehyde hexoside
			339.1079	$C_{16}H_{19}O_8^-$	339.1074	-1.5	
4	11.3	13.0	371.0975	$C_{16}H_{19}O_{10}^+$	371.0973	0.5	7,8-dihydroxy-6-methoxycoumarin hexoside (fraxetin hexoside)
			369.0827	$C_{16}H_{17}O_{10}^-$	369.0816	3.0	
5	12.1	14.7	407.0949	$C_{17}H_{20}O_{10}Na^+$	407.0949	0.0	7-hydroxy-6,8-dimethoxycoumarin hexoside (isofraxidin hexoside)
			383.0992	$C_{17}H_{19}O_{10}^-$	383.0973	5.0	
6	12.3	14.9	409.0893	$C_{17}H_{22}O_9K^+$	409.0895	-0.5	sinapyl aldehyde hexoside
			369.1194	$C_{17}H_{21}O_9^-$	369.1180	3.8	
7	13.0	16.4	209.0446	$C_{10}H_9O_5^+$	209.0445	0.5	7,8-dihydroxy-6-methoxycoumarin (fraxetin)
			207.0282	$C_{10}H_7O_5^-$	207.0288	-2.9	
8	14.5	20.0	193.0502	$C_{10}H_9O_4^+$	193.0495	3.6	7-hydroxy-6-methoxycoumarin (scopoletin)
			191.0341	$C_{10}H_7O_4^-$	191.0339	1.0	
9	14.8	21.6	223.0604	$C_{11}H_{11}O_5^+$	223.0601	1.3	7-hydroxy-6,8-dimethoxycoumarin (isofraxidin)
			221.0442	$C_{11}H_9O_5^-$	221.0445	-1.4	
10	15.6	23.0	195.0649	$C_{10}H_{11}O_4^+$	195.0652	-1.5	ferulic acid
			193.0504	$C_{10}H_9O_4^-$	193.0495	4.7	
11	15.6	23.8	223.0604	$C_{11}H_{11}O_5^+$	223.0601	1.3	6-hydroxy-5,7-dimethoxycoumarin (fraxinol)
			221.0442	$C_{11}H_9O_5^-$	221.0445	-1.4	
12	16.1	21.6	179.0708	$C_{10}H_{11}O_3^+$	179.0703	2.7	ferulic acid

Compound #	RT (min) program 1	RT (min) program 2	Measured <i>m/z</i>	Molecular formula	Calculated <i>m/z</i>	Error <i>m/z</i> (ppm)	Annotation
14	16.5	30.7	403.1018	C ₂₀ H ₁₉ O ₉ ⁺	403.1024	-1.5	5'-hydroxycleomiscosins A and/or B
			401.0877	C ₂₀ H ₁₇ O ₉ ⁻	401.0867	2.5	
15	18.0	35.5	417.1175	C ₂₁ H ₂₁ O ₉ ⁺	417.1180	-1.2	cleomiscosin D
			415.1022	C ₂₁ H ₁₉ O ₉ ⁻	415.1024	-0.5	
16	18.5	37.0	417.1173	C ₂₁ H ₂₁ O ₉ ⁺	417.1180	-1.7	cleomiscosin C
			415.1022	C ₂₁ H ₁₉ O ₉ ⁻	415.1024	-0.5	
17	18.5	37.0	387.1073	C ₂₀ H ₁₉ O ₈ ⁺	387.1074	-0.3	cleomiscosin B
			385.0930	C ₂₀ H ₁₇ O ₈ ⁻	385.0918	3.1	
18	19.0	38.6	387.1073	C ₂₀ H ₁₉ O ₈ ⁺	387.1074	-0.2	cleomiscosin A
			385.0922	C ₂₀ H ₁₇ O ₈ ⁻	385.0918	1.0	

Table 2. Phenolic compound standards used for identification purposes: retention times (RT), exact mass-to-charge ratios (m/z), molecular formulae and error m/z (in ppm). The m/z ratios of parent and fragment ions were determined from the data in the HPLC-ESI-MS(TOF) and HPLC-ESI-MS/MS(ion trap) chromatograms, respectively, working in both positive and negative mode. Common names for coumarins and their glucosides are indicated in brackets. The parent ion m/z ratios correspond to $[M+H]^+$ and $[M-H]^-$. The major ion of the MS² and MS³ spectra is indicated in bold.

Name	RT (min) program 2	Measured m/z	Molecular formula	Calculated m/z	Error m/z (ppm)	ESI-MS ⁿ m/z (Relative intensity, in %)
7-hydroxy-6-methoxycoumarin 7-glucoside (scopolin, scopoletin 7-O-glucoside)	10.3	355.1021	C ₁₆ H ₁₉ O ₉ ⁺	355.1024	-0.8	MS ² [355]: 337 (11), 245 (3), 193 (100) , 149 (1), 165 (1), 133 (12), 105 (5) MS ³ [355→193]: 178 (16), 165 (21), 149 (11), 137 (6), 133 (100)
		353.0876	C ₁₆ H ₁₇ O ₉ ⁻	353.0867	2.5	MS ² [353]: 191 (100) , 176 (9) MS ³ [353→191]: 176 (100)
7,8-dihydroxy-6- methoxycoumarin 8-glucoside (fraxin)	13.0	371.0956	C ₁₆ H ₁₉ O ₁₀ ⁺	371.0973	-4.6	MS ² [371]: 368 (11), 362 (13), 357 (12), 355 (66), 353 (35), 340 (13), 327 (23), 326 (25), 325 (195), 309 (15), 300 (17), 288 (10), 269 (19), 268 (11), 265 (11), 262 (14), 261 (17), 221 (12), 209 (100) , 187 (19), 177 (14), 170 (19), 156 (15), 133 (24) MS ³ [371→209]: 194 (100)
		369.0825	C ₁₆ H ₁₇ O ₁₀ ⁻	369.0816	2.4	MS ² [369]: 207 (100) , 192 (20) MS ³ [369→207]: 192 (100) , 163 (0.2)
7,8-dihydroxy-6- methoxycoumarin (fraxetin)	16.4	209.0444	C ₁₀ H ₉ O ₅ ⁺	209.0445	-0.5	MS ² [209]: 194 (31), 181 (52), 177 (15), 165 (7), 163 (80), 153(9), 149 (100) , 135 (13), 107 (18)
		207.0291	C ₁₀ H ₇ O ₅ ⁻	207.0288	1.4	MS ² [207]: 192 (100) , 163 (0.3)
7-hydroxy-6-methoxycoumarin (scopoletin)	20.0	193.0494	C ₁₀ H ₉ O ₄ ⁺	193.0495	-0.5	MS ² [193]: 178 (8), 165 (31), 149 (12), 137 (12), 133 (100) , 117 (2), 105 (3), 89 (3), 63 (6)
		191.0346	C ₁₀ H ₇ O ₄ ⁻	191.0339	3.7	MS ² [191]: 176 (100) , 148 (0.4)
7-hydroxy-6,8- dimethoxycoumarin (isofraxidin)	21.6	223.0594	C ₁₁ H ₁₁ O ₅ ⁺	223.0601	-3.1	MS ² [223]: 208 (100) , 207 (7), 195 (14), 191 (8), 190 (49), 179 (7), 163 (72), 162 (6), 135 (19) 107 (45)
		221.0443	C ₁₁ H ₉ O ₅ ⁻	221.0445	-0.9	MS ² [221]: 206 (100) , 209 (0.5), 191 (5), 162 (0.8)
ferulic acid	23.0	195.0657	C ₁₀ H ₁₁ O ₄ ⁺	195.0652	2.6	MS ² [195]: 177 (100) , 153 (4), 145 (3)
		193.0504	C ₁₀ H ₉ O ₄ ⁻	193.0495	4.7	MS ² [193]: 178 (70), 149 (100) , 139 (80)
6-hydroxy-5,7- dimethoxycoumarin (fraxinol)	23.8	223.0594	C ₁₁ H ₁₁ O ₅ ⁺	223.0601	-3.1	MS ² [223]: 208 (100) , 195 (11), 190 (40), 179 (6), 163 (54), 135 (19), 107 (39), 91 (4)
		221.0440	C ₁₁ H ₉ O ₅ ⁻	221.0444	-1.8	MS ² [221]: 206 (100) , 191 (5), 209 (0.5), 162 (0.2)
coniferyl aldehyde	24.6	179.0706	C ₁₀ H ₁₁ O ₃ ⁺	179.0703	1.7	MS ² [179]: 161 (100) , 147 (97), 133 (18), 119 (7), 105 (10)
		177.0554	C ₁₀ H ₉ O ₃ ⁻	177.0546	4.5	MS ² [177]: 162 (100) , 163 (1), 158 (0.3)
sinapyl aldehyde	25.1	209.0810	C ₁₁ H ₁₃ O ₄ ⁺	209.0808	1.0	MS ² [209]: 191 (47), 181 (10), 177 (100) , 153 (7), 149 (20), 145 (15), 131

Name	RT (min) program 2	Measured <i>m/z</i>	Molecular formula	Calculated <i>m/z</i>	Error <i>m/z</i> (ppm)	ESI-MS ⁿ <i>m/z</i> (Relative intensity, in %)
		207.0662	C ₁₁ H ₁₁ O ₄ ⁻	207.0652	4.8	(12), 121 (17), 103 (5) MS ² [207]: 192 (100) , 191 (0.3), 177 (2), 147 (0.2), 133 (0.2)

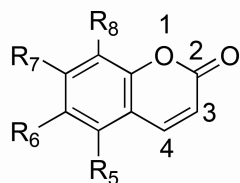
In review

Table 3. MS/MS data for some of the compounds secreted and accumulated by *Arabidopsis thaliana* roots in response to Fe deficiency: *m/z* ratios of the fragment ions and their relative intensity. Numbers in italics (Compound #) refer to the labels used for each compound in Table 1. All data were taken from the HPLC-ESI-MS/MS(ion trap) analysis. The major ion of the MS² and MS³ spectra is also indicated in bold.

<i>Compound #</i>	Annotation	Parent ion <i>m/z</i>	Ion type	ESI-MS ⁿ <i>m/z</i> (Relative intensity, in %)
3	coniferylaldehyde hexoside	339.1	[M-H] ⁻	MS ² [339]: 295 (6), 275 (8), 250 (6), 249 (3), 188 (3), 177 (100) , 162 (3) MS ³ [339→177]: 162 (100)
4	7,8-dihydroxy-6-methoxycoumarin hexoside (fraxetin hexoside)	369.1	[M-H] ⁻	MS ² [369]: 325 (7), 323 (5), 223 (11), 215 (8), 207 (100) , 193 (5), 192 (20) MS ³ [369→207]: 192 (100)
5	7-hydroxy-6,8-dimethoxycoumarin hexoside (isofraxidin hexoside)	383.1	[M-H] ⁻	MS ² [383]: 365 (13), 347 (24), 341 (12), 339 (10), 337 (22), 323 (24), 322 (18), 303 (14), 270 (20), 268 (25), 266 (18), 252 (9), 251 (30), 221 (100) , 215 (38), 207 (7), 206 (11), 203 (11), 199 (15), 187 (8), 177 (20), 173(8), 156 (11), 131 (17), 129 (30), 125 (6), 114 (24) MS ³ [383→221]: 206 (100)
6	sinapyl aldehyde hexoside	369.1	[M-H] ⁻	MS ² [369]: 351 (33), 325 (11), 289 (10), 254 (5), 253 (6), 246 (11), 245 (8), 239 (9), 237 (11), 217 (6), 207 (100) , 192 (18), 159 (11), 128 (10) MS ³ [369→207]: 192 (100)
10	ferulic acid	193.1	[M-H] ⁻	MS ² [193]: 178 (70), 149 (100) , 134 (72)
12	coniferyl aldehyde	179.1	[M+H] ⁺	MS ² [179]: 161 (86), 147 (100) , 133 (17), 119 (10), 105 (8)
13	sinapyl aldehyde	209.1	[M+H] ⁺	MS ² [209]: 191 (41), 181 (17), 177 (100) , 149 (22), 145 (13), 131 (5), 121 (18)

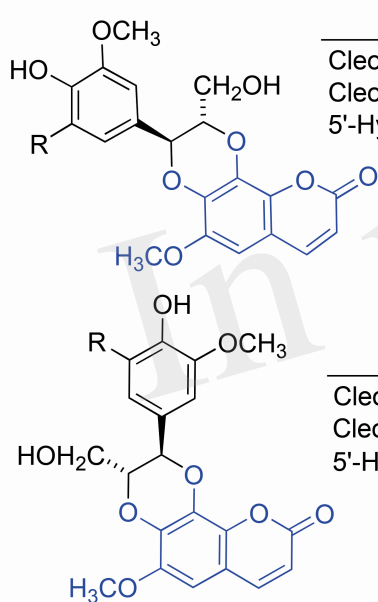
Figure 1.TIFF

a)



Name	R ₅	R ₆	R ₇	R ₈
Esculetin	H	OH	OH	H
Esculin	H	O-Glucose	OH	H
Scopoletin	H	OCH ₃	OH	H
Scopolin	H	OCH ₃	O-Glucose	H
Fraxetin	H	OCH ₃	OH	OH
Fraxin	H	OCH ₃	OH	O-Glucose
Isofraxidin	H	OCH ₃	OH	OCH ₃
Fraxinol	OCH ₃	OH	OCH ₃	H

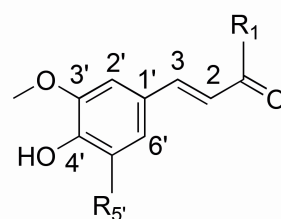
c)



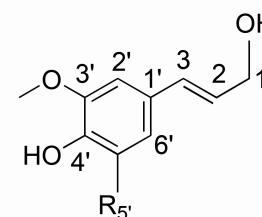
Name	R
Cleomiscosin A	H
Cleomiscosin C	OCH ₃
5'-Hydroxycleomiscosin A	OH

Name	R
Cleomiscosin B	H
Cleomiscosin D	OCH ₃
5'-Hydroxycleomiscosin B	OH

b)



Name	R ₁	R _{5'}
Coniferyl aldehyde	H	H
Ferulic acid	OH	H
Sinapyl aldehyde	H	OCH ₃



Name	R _{5'}
Coniferyl alcohol	H
Hydroxyconiferyl alcohol	OH
Sinapyl alcohol	OCH ₃

d)

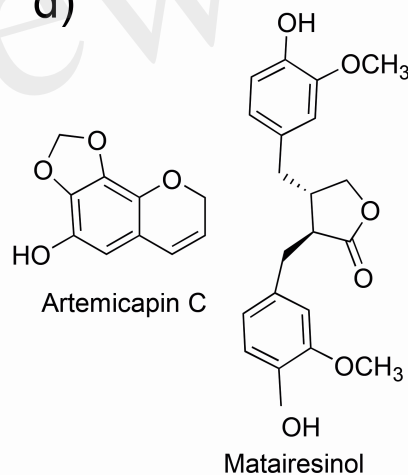


Figure 2.TIFF

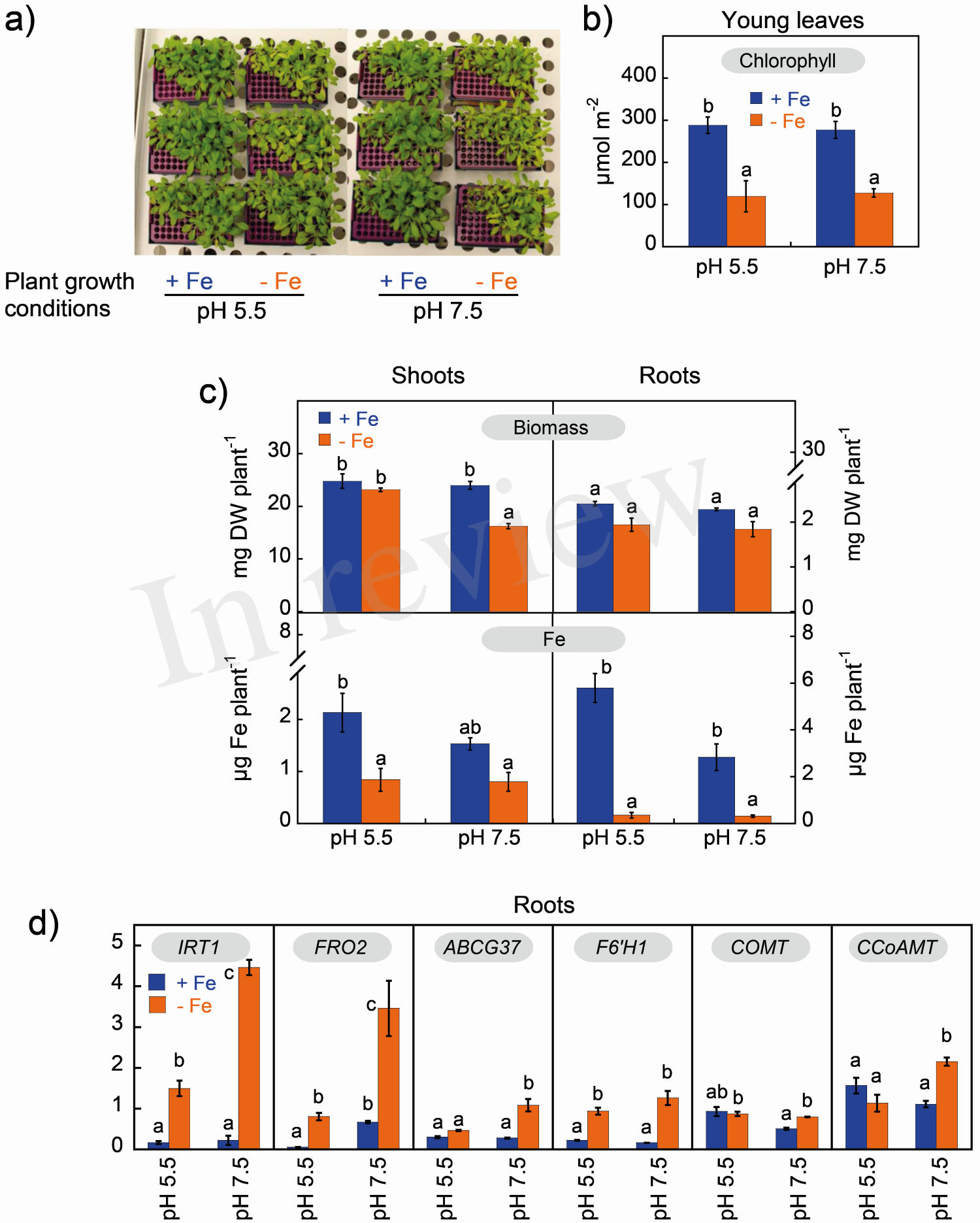


Figure 3.TIFF

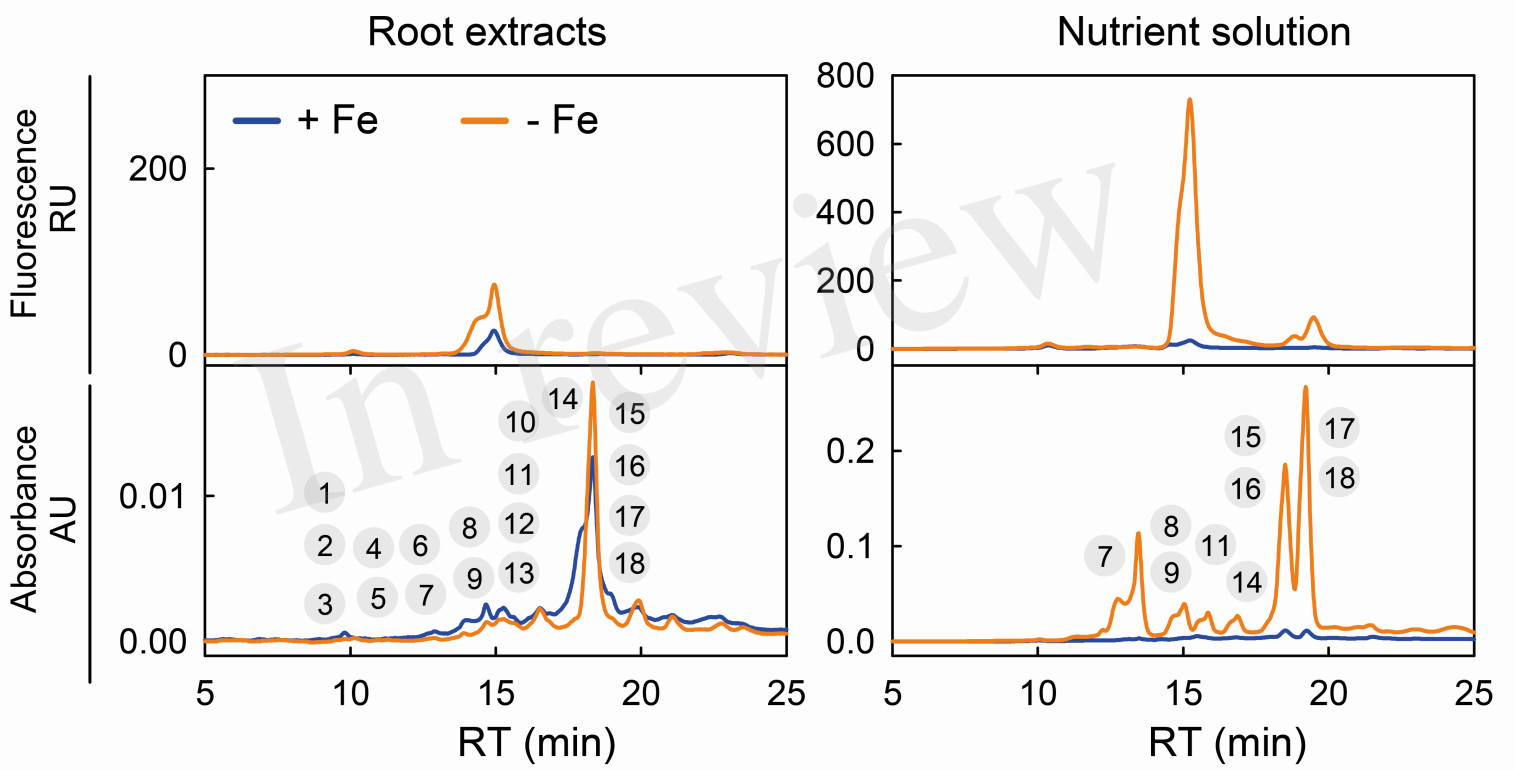


Figure 4.TIF

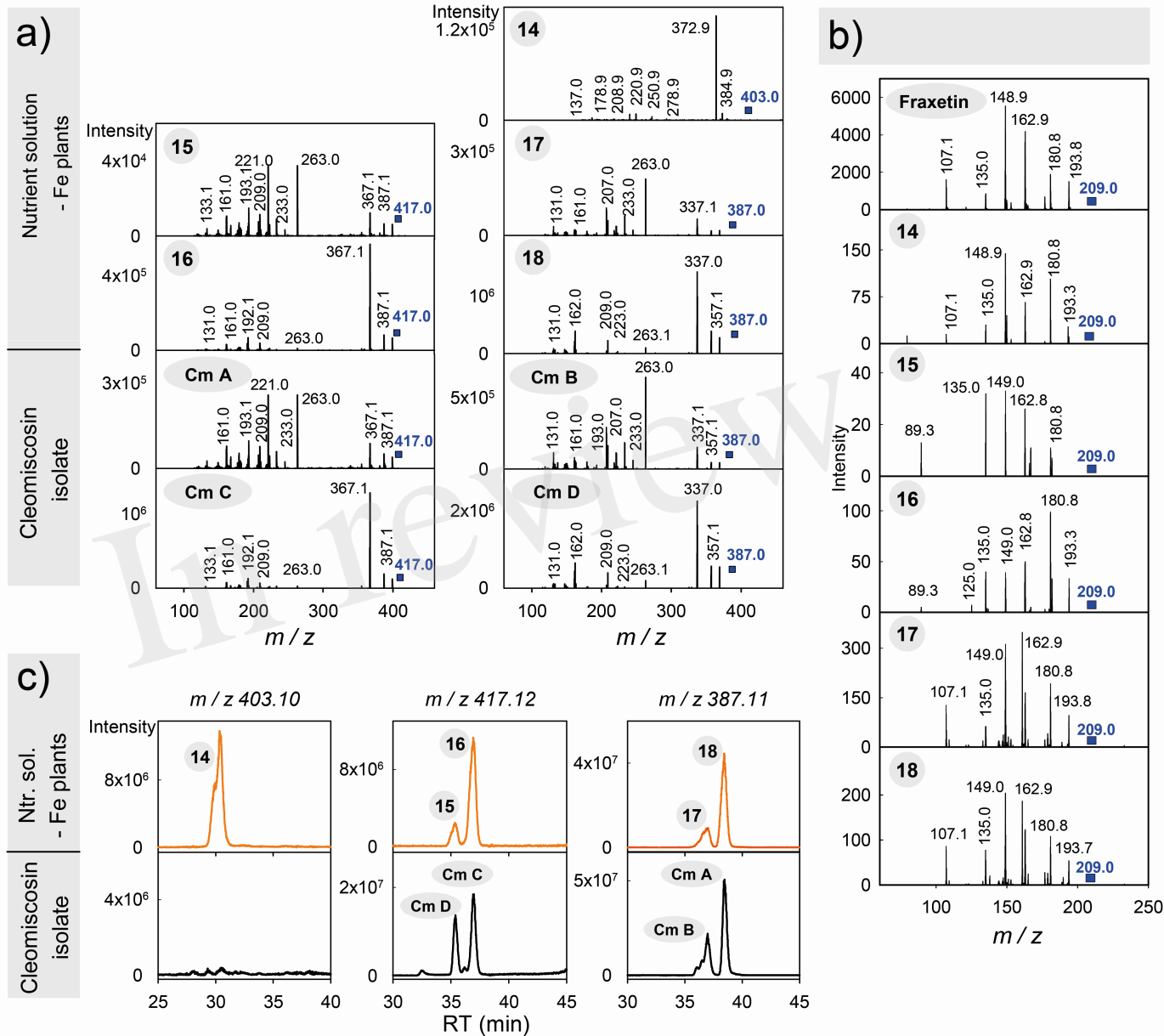


Figure 5.TIFF

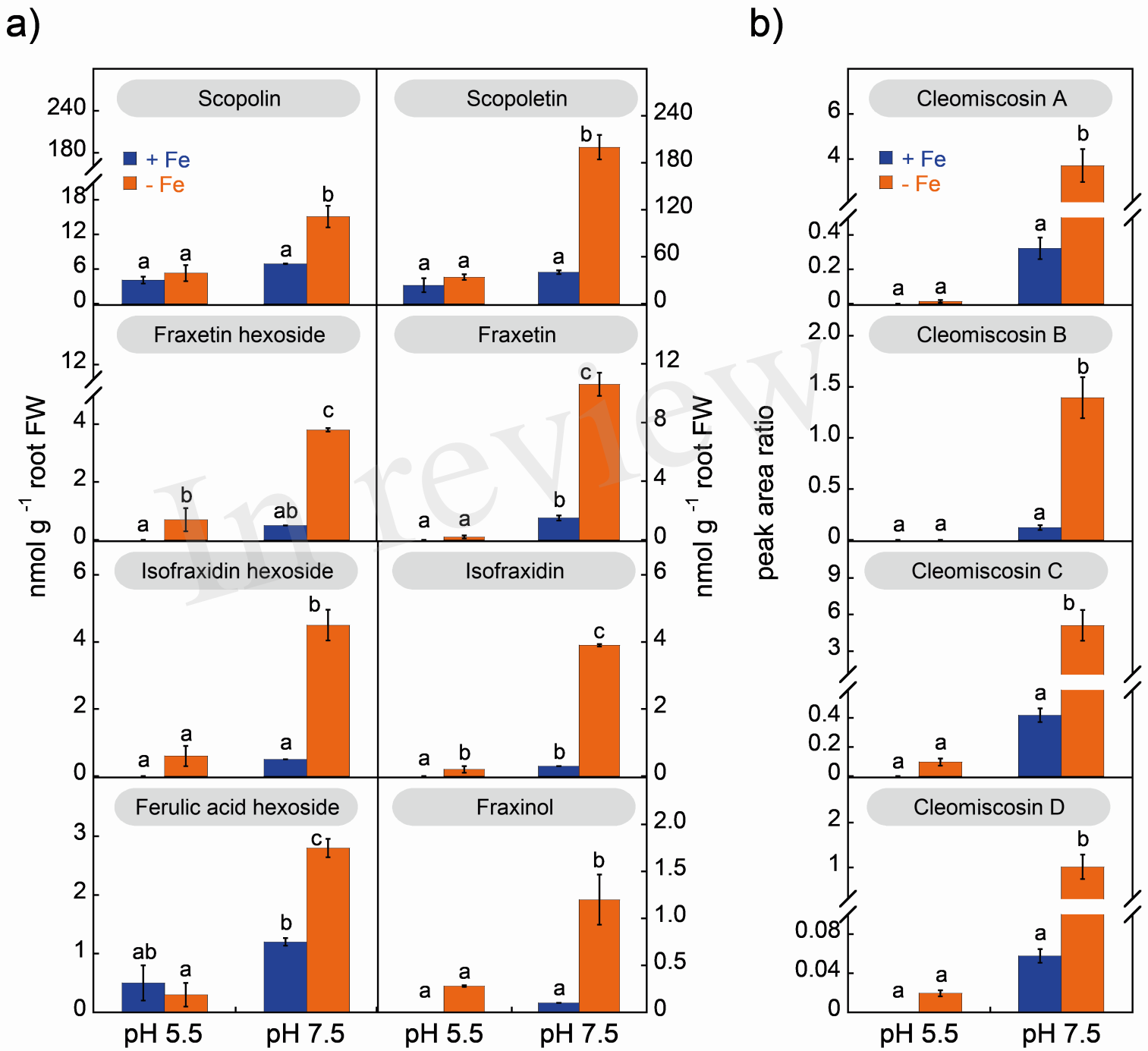


Figure 6.TIFF

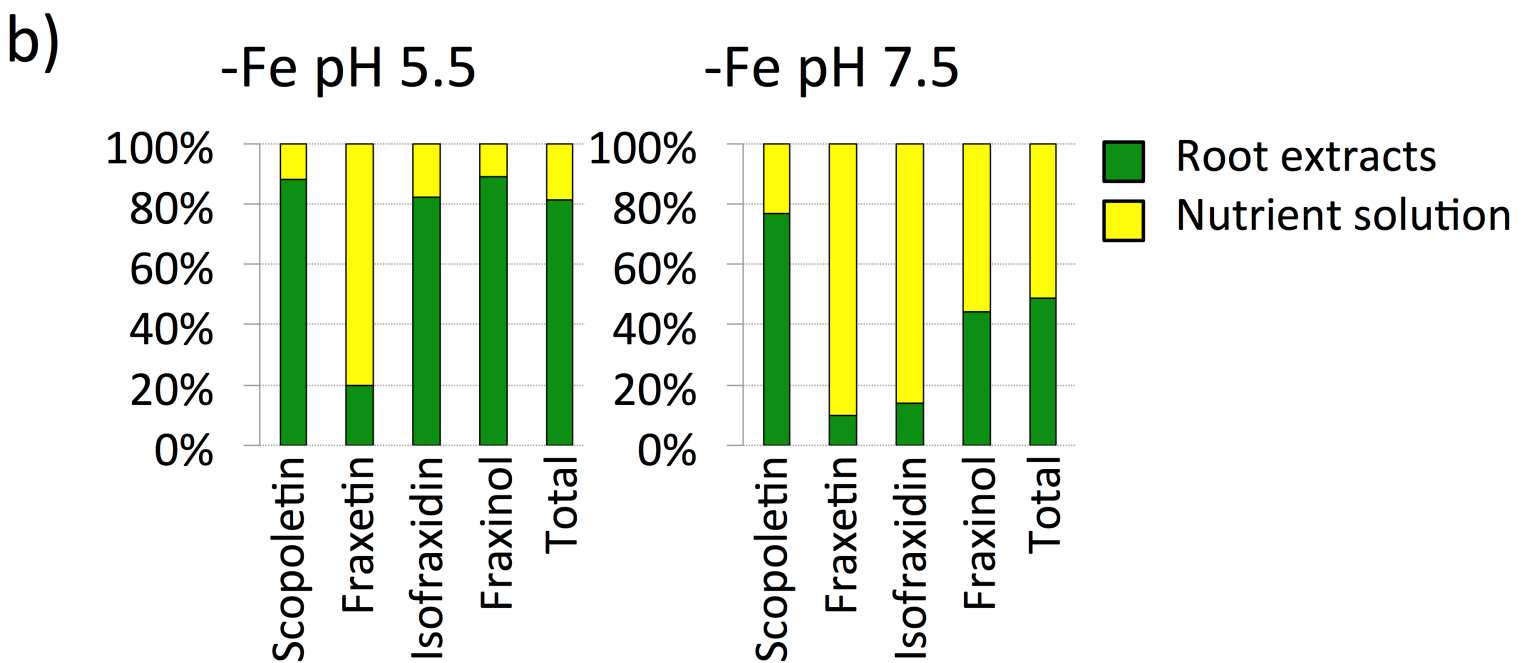
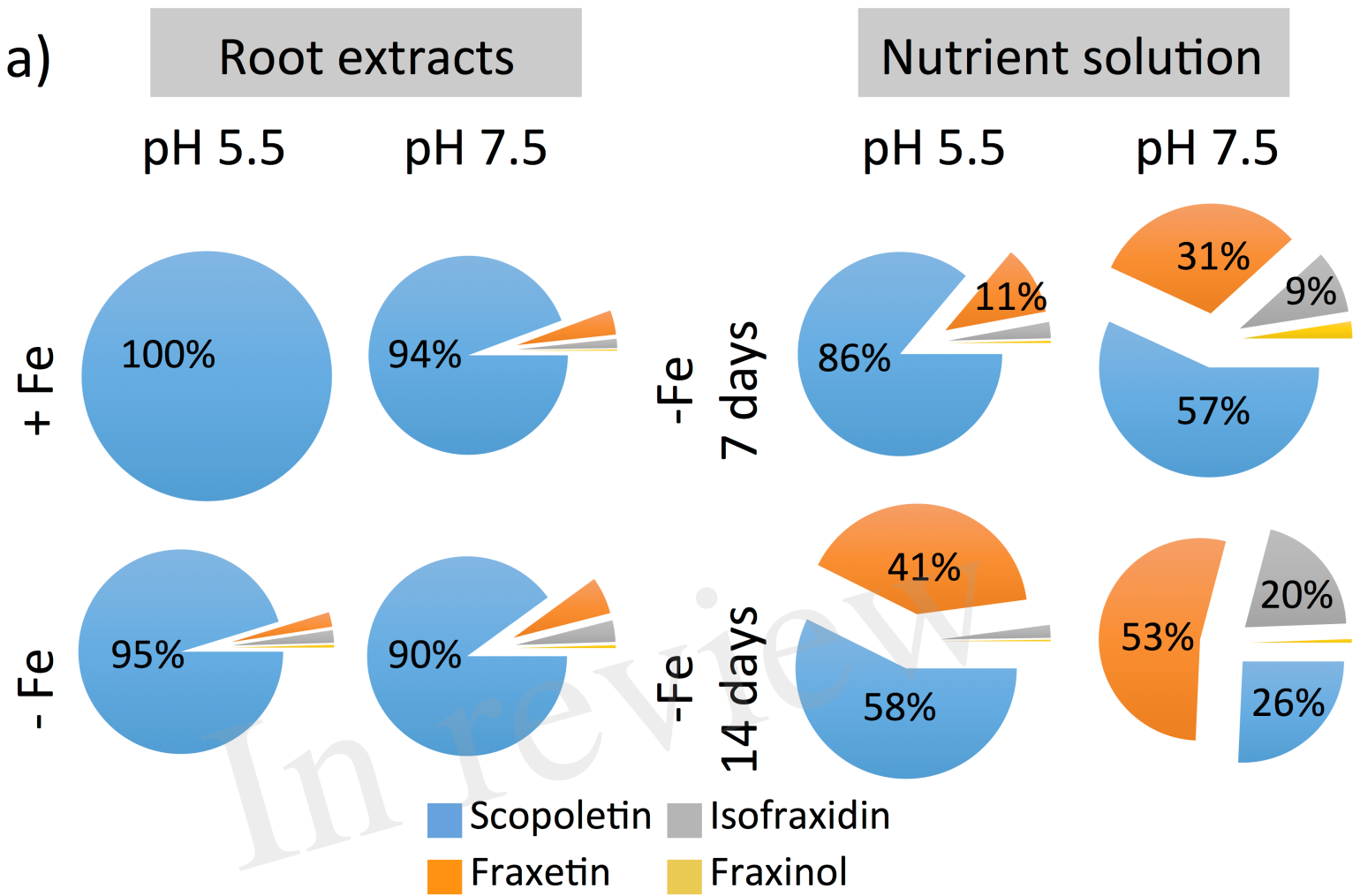
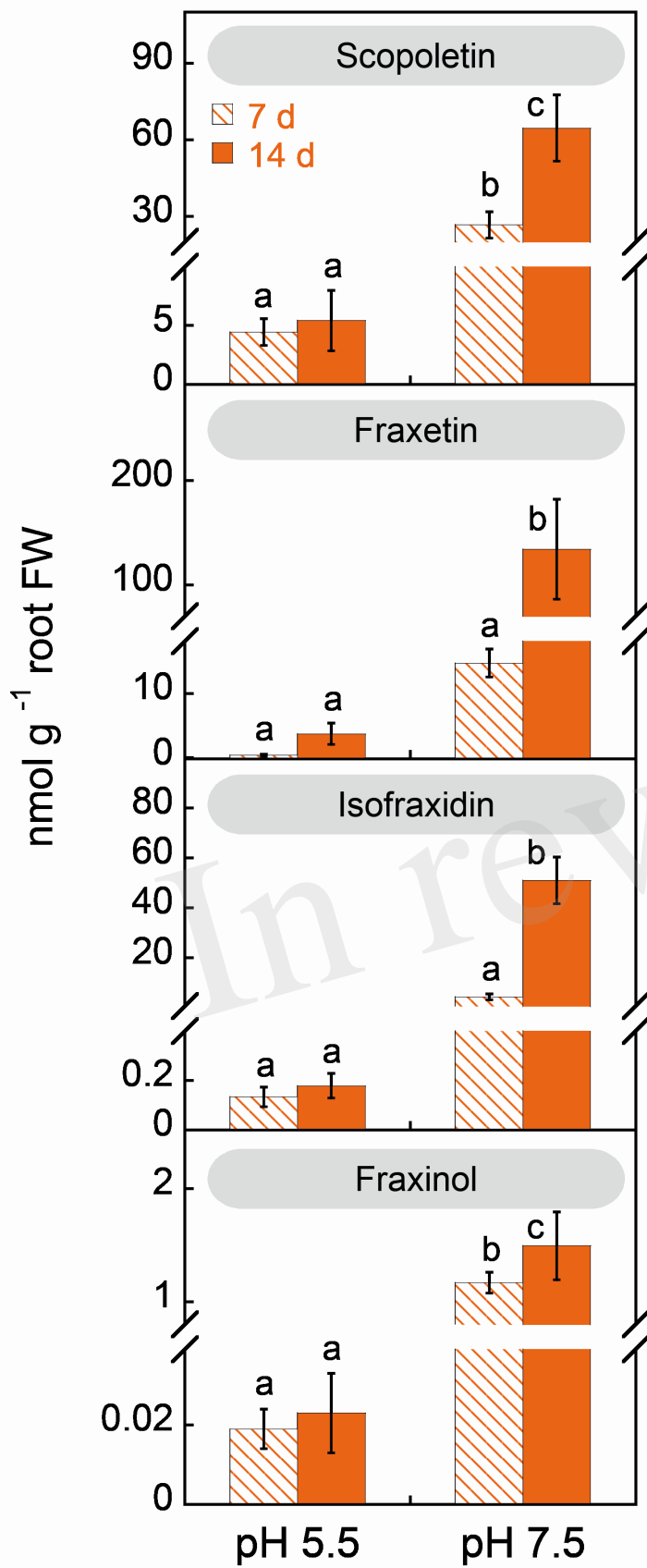


Figure 7.TIFF

a)



b)

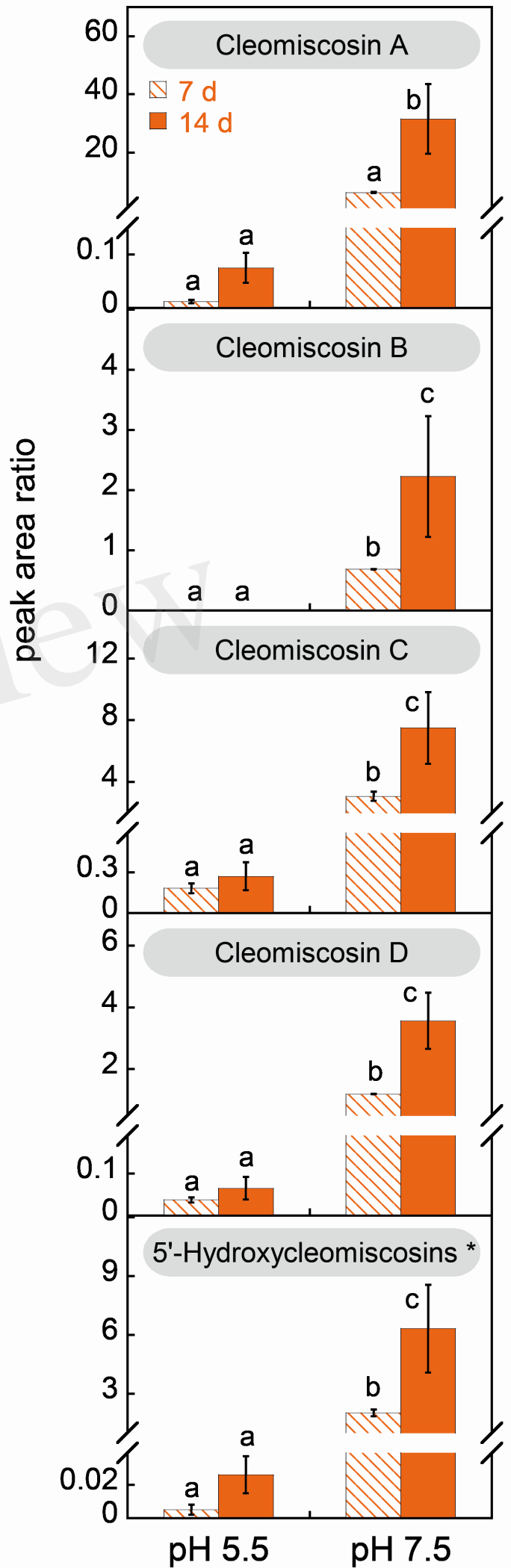


Figure 8.TIF

